

NUCLEAR DATA AND MEASUREMENTS SERIES

ANL/NDM-56

Fast-Neutron Interactions with ^{182}W , ^{184}W , and ^{186}W

by

P.T. Guenther, A.B. Smith, and J.F. Whalen

June 1981

**ARGONNE NATIONAL LABORATORY,
ARGONNE, ILLINOIS 60439, U.S.A.**

NUCLEAR DATA AND MEASUREMENTS SERIES

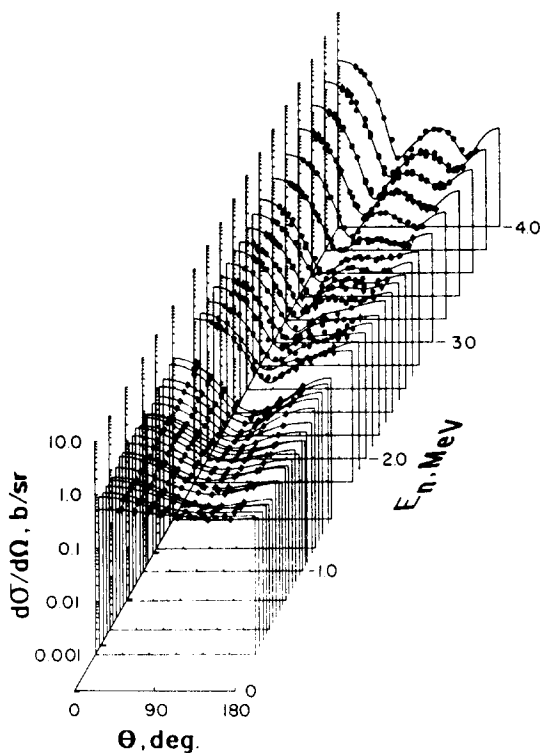
ANL/NDM-56

FAST-NEUTRON INTERACTIONS WITH ^{182}W , ^{184}W and ^{186}W

by

P. T. Guenther, A. B. Smith and J. F. Whalen

June 1981



U of C - AUA - USDOE

ARGONNE NATIONAL LABORATORY,
ARGONNE, ILLINOIS 60439, U.S.A.

The facilities of Argonne National Laboratory are owned by the United States Government. Under the terms of a contract (W-31-109-Eng-38) between the U. S. Department of Energy, Argonne Universities Association and The University of Chicago, the University employs the staff and operates the Laboratory in accordance with policies and programs formulated, approved and reviewed by the Association.

MEMBERS OF ARGONNE UNIVERSITIES ASSOCIATION

The University of Arizona	Kansas State University	The Ohio State University
Carnegie-Mellon University	The University of Kansas	Ohio University
Case Western Reserve University	Loyola University	The Pennsylvania State University
The University of Chicago	Marquette University	Purdue University
University of Cincinnati	Michigan State University	Saint Louis University
Illinois Institute of Technology	The University of Michigan	Southern Illinois University
University of Illinois	University of Minnesota	The University of Texas at Austin
Indiana University	University of Missouri	Washington University
Iowa State University	Northwestern University	Wayne State University
The University of Iowa	University of Notre Dame	The University of Wisconsin

NOTICE

This report was prepared as an account of work sponsored by the United States Government. Neither the United States nor the United States Department of Energy, nor any of their employees, nor any of their contractors, subcontractors, or their employees, makes any warranty, express or implied, or assumes any legal liability or responsibility for the accuracy, completeness or usefulness of any information, apparatus, product or process disclosed, or represents that its use would not infringe privately-owned rights. Mention of commercial products, their manufacturers, or their suppliers in this publication does not imply or connote approval or disapproval of the product by Argonne National Laboratory or the U. S. Department of Energy.

ANL/NDM-56

FAST-NEUTRON INTERACTIONS WITH ^{182}W , ^{184}W and ^{186}W

by

P. T. Guenther, A. B. Smith and J. F. Whalen

June 1981

Applied Physics Division
Argonne National Laboratory
9700 South Cass Avenue
Argonne, Illinois 60439
USA

NUCLEAR DATA AND MEASUREMENTS SERIES

The Nuclear Data and Measurements Series presents results of studies in the field of microscopic nuclear data. The primary objective is the dissemination of information in the comprehensive form required for nuclear technology applications. This Series is devoted to: a) measured microscopic nuclear parameters, b) experimental techniques and facilities employed in measurements, c) the analysis, correlation and interpretation of nuclear data, and d) the evaluation of nuclear data. Contributions to this Series are reviewed to assure technical competence and, unless otherwise stated, the contents can be formally referenced. This Series does not supplant formal journal publication but it does provide the more extensive information required for technological applications (e.g., tabulated numerical data) in a timely manner.

OTHER ISSUES IN THE ANL/NDM SERIES ARE:

- ANL/NDM-1 Cobalt Fast Neutron Cross Sections-Measurement and Evaluation by P. T. Guenther, P. A. Moldauer, A. B. Smith, D. L. Smith and J. F. Whalen, July 1973.
- ANL/NDM-2 Prompt Air-Scattering Corrections for a Fast-Neutron Fission Detector: $E_n \leq 5$ MeV by Donald L. Smith, September 1973.
- ANL/NDM-3 Neutron Scattering from Titanium; Compound and Direct Effects by E. Barnard, J. deVilliers, P. Moldauer, D. Reitmann, A. Smith and J. Whalen, October 1973.
- ANL/NDM-4 ^{90}Zr and ^{92}Zr ; Neutron Total and Scattering Cross Sections by P. Guenther, A. Smith and J. Whalen, July 1974.
- ANL/NDM-5 Delayed Neutron Data - Review and Evaluation by Samson A. Cox, April 1974.
- ANL/NDM-6 Evaluated Neutronic Cross Section File for Niobium by R. Howerton, Lawrence Livermore Laboratory and A. Smith, P. Guenther and J. Whalen, Argonne National Laboratory, May 1974.
- ANL/NDM-7 Neutron Total and Scattering Cross Sections of Some Even Isotopes of Molybdenum and the Optical Model by A. B. Smith, P. T. Guenther and J. F. Whalen, June 1974.
- ANL/NDM-8 Fast Neutron Capture and Activation Cross Sections of Niobium Isotopes by W. P. Poenitz, May 1974.
- ANL/NDM-9 Method of Neutron Activation Cross Section Measurement for $E_n = 5.5\text{--}10$ MeV Using the D(d,n)He-3 Reaction as a Neutron Source by D. L. Smith and J. W. Meadows, August 1974.
- ANL/NDM-10 Cross Sections for (n,p) Reactions on ^{27}Al , $^{46,47,48}\text{Ti}$, $^{54,56}\text{Fe}$, ^{58}Ni , ^{59}Co and ^{64}Zn from Near Threshold to 10 MeV by Donald L. Smith and James W. Meadows, January 1975.
- ANL/NDM-11 Measured and Evaluated Fast Neutron Cross Sections of Elemental Nickel by P. Guenther, A. Smith, D. Smith and J. Whalen, Argonne National Laboratory and R. Howerton, Lawrence Livermore Laboratory, July 1975.
- ANL/NDM-12 A Spectrometer for the Investigation of Gamma Radiation Produced by Neutron-Induced Reactions by Donald L. Smith, April 1975.
- ANL/NDM-13 Response of Several Threshold Reactions in Reference Fission Neutron Fields by Donald L. Smith and James W. Meadows, June 1975.
- ANL/NDM-14 Cross Sections for the $^{66}\text{Zn(n,p)}^{66}\text{Cu}$, $^{113}\text{In(n,n')}^{113\text{m}}\text{In}$ and $^{115}\text{In(n,n')}^{115\text{m}}\text{In}$ Reactions from Near Threshold to 10 MeV by Donald L. Smith and James W. Meadows, July 1975.

- ANL/NDM-15 Radiative Capture of Fast Neutrons in ^{165}Ho and ^{181}Ta by W. P. Poenitz, June 1975.
- ANL/NDM-16 Fast Neutron Excitation of the Ground-State Rotational Band of ^{238}U by P. Guenther, D. Havel and A. Smith, September 1975.
- ANL/NDM-17 Sample-Size Effects in Fast-Neutron Gamma-Ray Production Measurements: Solid-Cylinder Samples by Donald L. Smith, September 1975.
- ANL/NDM-18 The Delayed Neutron Yield of ^{238}U and ^{241}Pu by J. W. Meadows January 1976.
- ANL/NDM-19 A Remark on the Prompt-Fission-Neutron Spectrum of ^{252}Cf by P. Guenther, D. Havel, R. Sjoblom and A. Smith, March 1976.
- ANL/NDM-20 Fast-Neutron-Gamma-Ray Production from Elemental Iron: $E_n \lesssim 2$ MeV by Donald L. Smith, May 1976.
- ANL/NDM-21 Note on the Experimental Determination of the Relative Fast-Neutron Sensitivity of a Hydrogenous Scintillator by A. Smith, P. Guenther and R. Sjoblom, June 1976.
- ANL/NDM-22 Note on Neutron Scattering and the Optical Model Near $A=208$ by P. Guenther, D. Havel and A. Smith, September 1976.
- ANL/NDM-23 Remarks Concerning the Accurate Measurement of Differential Cross Sections for Threshold Reactions Used in Fast-Neutron Dosimetry for Fission Reactors by Donald L. Smith, December 1976.
- ANL/NDM-24 Fast Neutron Cross Sections of Vanadium and an Evaluated Neutronic File by P. Guenther, D. Havel, R. Howerton, F. Mann, D. Smith, A. Smith and J. Whalen, May 1977.
- ANL/NDM-25 Determination of the Energy Scale for Neutron Cross Section Measurements Employing a Monoenergetic Accelerator by J. W. Meadows, January 1977.
- ANL/NDM-26 Evaluation of the $\text{IN-115}(\text{N},\text{N}')\text{IN-115M}$ Reaction for the ENDF/B-V Dosimetry File by Donald L. Smith, December 1976.
- ANL/NDM-27 Evaluated (n,p) Cross Sections of ^{46}Ti , ^{47}Ti and ^{48}Ti by C. Philis and O. Bersillon, Bruyeres-le-Chatel, France and D. Smith and A. Smith, Argonne National Laboratory, January 1977.
- ANL/NDM-28 Titanium-II: An Evaluated Nuclear Data File by C. Philis, Centre d'Etudes de Bruyères-le-Châtel, R. Howerton, Lawrence Livermore Laboratory and A. B. Smith, Argonne National Laboratory, June 1977.
- ANL/NDM-29 Note on the 250 keV Resonance in the Total Neutron Cross Section of ^6Li by A. B. Smith, P. Guenther, D. Havel and J. F. Whalen, June 1977.

- ANL/NDM-30 Analysis of the Sensitivity of Spectrum-Average Cross Sections to Individual Characteristics of Differential Excitation Functions by Donald L. Smith, March 1977.
- ANL/NDM-31 Titanium-I: Fast Neutron Cross Section Measurements by P. Guenther, D. Havel, A. Smith and J. Whalen, May 1977.
- ANL/NDM-32 Evaluated Fast Neutron Cross Section of Uranium-238 by W. Poenitz, E. Pennington, and A. B. Smith, Argonne National Laboratory and R. Howerton, Lawrence Livermore Laboratory, October 1977.
- ANL/NDM-33 Comments on the Energy-Averaged Total Neutron Cross Sections of Structural Materials by A. B. Smith and J. F. Whalen, June 1977.
- ANL/NDM-34 Graphical Representation of Neutron Differential Cross Section Data for Reactor Dosimetry Applications by Donald L. Smith, June 1977.
- ANL/NDM-35 Evaluated Nuclear Data File of Th-232 by J. Meadows, W. Poenitz, A. Smith, D. Smith and J. Whalen, Argonne National Laboratory and R. Howerton, Lawrence Livermore Laboratory, February 1978.
- ANL/NDM-36 Absolute Measurements of the $^{233}\text{U}(n,f)$ Cross Section Between 0.13 and 8.0 MeV by W. P. Poenitz, April 1978.
- ANL/NDM-37 Neutron Inelastic Scattering Studies for Lead-204 by D. L. Smith and J. W. Meadows, December 1977.
- ANL/NDM-38 The Alpha and Spontaneous Fission Half-Lives of ^{242}Pu by J. W. Meadows, December 1977.
- ANL/NDM-39 The Fission Cross Section of ^{239}Pu Relative to ^{235}U from 0.1 to 10 MeV by J. W. Meadows, March 1978.
- ANL/NDM-40 Statistical Theory of Neutron Nuclear Reactions by P. A. Moldauer, February 1978.
- ANL/NDM-41 Energy-Averaged Neutron Cross Sections of Fast-Reactor Structural Materials by A. Smith, R. McKnight and D. Smith, February 1978.
- ANL/NDM-42 Fast Neutron Radiative Capture Cross Section of ^{232}Th by W. P. Poenitz and D. L. Smith, March 1978.
- ANL/NDM-43 Neutron Scattering from ^{12}C in the Few-MeV Region by A. Smith, R. Holt and J. Whalen, September 1978.
- ANL/NDM-44 The Interaction of Fast Neutrons with ^{60}Ni by A. Smith, P. Guenther, D. Smith and J. Whalen, January 1979.
- ANL/NDM-45 Evaluation of $^{235}\text{U}(n,f)$ between 100 KeV and 20 MeV by W. P. Poenitz, July 1979.

- ANL/NDM-46 Fast-Neutron Total and Scattering Cross Sections of ^{107}Ag in the MeV Region by A. Smith, P. Guenther, G. Winkler and J. Whalen, January 1979.
- ANL/NDM-47 Scattering of MeV Neutrons from Elemental Iron by A. Smith and P. Guenther, March 1979.
- ANL/NDM-48 ^{235}U Fission Mass and Counting Comparison and Standardization by W. P. Poenitz, J. W. Meadows and R. J. Armani, May 1979.
- ANL/NDM-49 Some Comments on Resolution and the Analysis and Interpretation of Experimental Results from Differential Neutron Measurements by Donald L. Smith, November 1979.
- ANL/NDM-50 Prompt-Fission-Neutron Spectra of ^{233}U , ^{235}U , ^{239}Pu and ^{240}Pu Relative to that of ^{252}Cf by A. Smith, P. Guenther, G. Winkler and R. McKnight, September 1979.
- ANL/NDM-51 Measured and Evaluated Neutron Cross Sections of Elemental Bismuth by A. Smith, P. Guenther, D. Smith and J. Whalen, April 1980.
- ANL/NDM-52 Neutron Total and Scattering Cross Sections of ^6Li in the Few MeV Region by P. Guenther, A. Smith and J. Whalen, February 1980.
- ANL/NDM-53 Neutron Source Investigations in Support of the Cross Section at the Argonne Fast-Neutron Generator by James W. Meadows and Donald L. Smith, May 1980.
- ANL/NDM-54 The Nonelastic-Scattering Cross Sections of Elemental Nickel by A. B. Smith, P. T. Guenther and J. F. Whalen, June 1980.
- ANL/NDM-55 Thermal Neutron Calibration of a Tritium Extraction Facility using the $^6\text{Li}(n,t)^4\text{He}/^{197}\text{Au}(n,\gamma)^{198}\text{Au}$ Cross Section Ratio for Standardization by M. M. Bretscher and D. L. Smith, August 1980.

TABLE OF CONTENTS

	<u>Page</u>
LIST OF FIGURES.....	viii
LIST OF TABLES.....	xiv
ABSTRACT.....	xv
I. INTRODUCTION.....	1
II. EXPERIMENTAL METHODS.....	3
A. Samples.....	3
B. Neutron Total-cross-section Measurements.....	4
C. Neutron Scattering Measurements.....	4
III. EXPERIMENTAL RESULTS.....	7
A. Neutron Total Cross Sections.....	7
B. Elastic Neutron Scattering.....	8
C. Neutron Inelastic Scattering.....	10
IV. PHYSICAL INTERPRETATION.....	45
V. EVALUATED NUCLEAR DATA FILE.....	73
A. Neutron Total Cross Sections.....	73
B. Elastic-neutron-scattering Cross Sections.....	74
C. Neutron inelastic-scattering Cross Sections.....	75
D. An Illustrative Comparison with ENDF/B-V.....	77
VI. CONCLUDING REMARKS.....	86
ACKNOWLEDGEMENTS.....	87
APPENDIX.....	88

LIST OF FIGURES

	<u>Page</u>
<u>Figure Captions, Section III.....</u>	<u>17</u>
Fig. III-1A. Neutron total-cross-section self-shielding correction factors for ^{186}W . Vertical axis gives the correction factor, the horizontal axis the sample thickness in nuclei/barn (n/b). Curves correspond to various neutron energies distributed from 100 to 500 keV. One and two cm sample thicknesses are noted by arrows.....	19
Fig. III-1B. Relative fully-corrected measured neutron total cross sections of elemental tungsten at illustrative energies of 98, 325 and 475 keV as a function of sample thickness given in nuclei/barn (n/b). Error bars indicate experimental statistical accuracies.....	19
Fig. III-2. Neutron total cross sections of ^{182}W , ^{184}W and ^{186}W . The present experimental results are indicated by data points. Curves denote averages of previously reported experimental results referenced as follows: A = 10 keV average of Ref. III-2, B = 100 keV average of Ref. III-3, and C = 100 keV average of Ref. III-4.....	20
Fig. III-3. Neutron time-of-flight spectrum obtained by scattering 1.8 MeV neutrons from ^{186}W at an angle of 115 deg. (Histogram). The flight-path was 5.5 m. The smooth curve indicates the result of fitting two gaussian distributions to the measured values corresponding to the elastic- and inelastic-(observed $E_x = 122$ keV) neutron groups.....	21
Fig. III-4. Representative ^{186}W time-of-flight spectra obtained at an incident energy of 3.0 MeV with a flight path of ≈ 20 m. Scattering angles are noted on the individual figures. The elastically-scattered neutron group is to the right of each figure, the inelastic group ($E_x \approx 121$ keV) to the left. All distributions are normalized to the same maximum heights. Small ($\approx 5\%$) backgrounds have been subtracted. Maximum events per unit time vary from several times 10^3 to several times 10^2	22
Fig. III-5. Measured differential-neutron-elastic-scattering cross sections of ^{182}W (A), ^{184}W (B) and ^{186}W (C). Data points indicate the measured values and curves the results of least-square fitting Eq. III-1 to the measured results as described in the text. (Cross-sections are given in b/sr and scattering angle in laboratory degrees.).....	23,24,25

LIST OF FIGURES (Contd.)

	Page
<u>Figure Captions, Section III. (Contd.)</u>	17
Fig. III-6. Measured neutron elastic-scattering (circular symbols) and total (crosses) cross sections of ^{182}W , ^{184}W and ^{186}W . The elastic scattering values at energies below 1.5 MeV were taken from Ref. III-7. Curves are "eye-guides" described in Sec. V of the text.....	26
Fig. III-7. Illustrative measured neutron differential-elastic-scattering cross sections of $^{182}\text{W(A)}$, $^{184}\text{W(B)}$ and $^{186}\text{W(C)}$. The present experimental results are noted by circular data points, those of Ref. III-8 by crosses. Curves denote the results of a least-square fit of Eq. III-1 to the present measured values as described in the text. Incident neutron energies are numerically given in MeV (cross sections are in b/sr and scattering angle in laboratory degrees).....	27,28,29
Fig. III-8. Representative TOF spectra for ^{186}W at several incident energies. Primed quantities indicate scattering from the second source-reaction group. Incident energies (MeV) and specific observed excitation energies (keV) are numerically noted. Plural scattering is also indicated. The inelastic neutron groups are emphasized with gaussian eye-guides. The gradual loss of resolution, as well as the increased complexity of the spectra, with incident energy is evident...	30
Fig. III-9. Excitations observed in the present neutron scattering experiments (boxes) compared with the level structure given in the compilation of Ref. III-9. Reported excitation energies in MeV and J^π values are given to excitations of ≈ 1.2 MeV. More details of the structure information are given in Ref. III-9.....	31
Fig. III-10. Angular distributions of neutrons resulting from the excitation of the 2+ member of the ground-state rotational band of ^{182}W , ^{184}W and ^{186}W . Measured values are indicated by data points. Curves denote the results of a least-square fit of Eq. III-1 to the measured values. Scattering angle is given in lab-degrees and cross section in b/sr.....	32
Fig. III-11. Angular distributions of neutrons resulting from the excitation of the 4+ member of the ground-state rotational band of ^{182}W , ^{184}W and ^{186}W . Notation is identical to that of Fig. III-10.....	33

LIST OF FIGURES (Contd.)

Page

Figure Captions, Section III. (Contd.).....17

Fig. III-12. Inelastic-neutron-scattering excitation cross sections of; (A) ^{182}W , (B) ^{184}W , and (C) ^{186}W . Circular data points indicate measured values where those at energies of less than 1.5 MeV are taken from Ref. III-6. Crossed data points indicate measured results combined with the previous (and lower energy) excitation. Observed excitation energies are numerically given in keV. Curves are "eye-guides" constructed through the measured values.....34,37,40

Fig. III-13. Some illustrative differential-neutron-scattering cross sections of the ^{186}W at an incident neutron energy of 3.0 MeV. Data points indicate measured values with excitations given in keV. Curves are the results of least square fitting procedures as described in the text. Scattering angle is given in lab-degrees and cross section in b/sr.....43

Fig. III-14. Comparison of measured cross sections for the excitation of the 2+ and 4+ states of the ground-state rotational bands of ^{182}W , ^{184}W and ^{186}W . Circular data points indicate the results of the present work at an incident energy of 3.5 MeV, crosses the results of Delaroche et al. (III-9) at an energy of 3.4 MeV. Cross section is given in b/sr and scattering angle in lab.-deg.....44

Figure Captions, Section IV.55

Fig. IV-1. Comparison of measured and calculated neutron cross sections of ^{182}W , ^{184}W and ^{186}W . The present measured values are indicated by data symbols as follows: + = total cross sections, 0 = elastic scattering, \square = inelastic excitation of the first 2+ state and X = inelastic excitation of the first 4+ state. The light "B" curve is an eye-guide constructed through the experimental results of Ref. IV-9 as described in the text. Heavy curves denote the results of calculations; "A" (or unmarked) are results obtained with the "base" model described in the text and "C" are results obtained with modified compound-nucleus corrections as defined in the text.....58

Fig. IV-2. Comparison of measured and calculated neutron differential-elastic-scattering cross sections of ^{182}W , ^{184}W and ^{186}W . Experimental results are indicated by data points and the results of calculations using the "base" model of the text by curves.....59

LIST OF FIGURES (Contd.)

	<u>Page</u>
<u>Figure Captions, Section IV. (Contd.)</u>	55
Fig. IV-3. Comparison of measured and calculated neutron-differential-scattering cross sections for the excitation of the first 2+ states of ^{182}W , ^{184}W and ^{186}W . The experimental results are indicated by data symbols and those obtained via calculation by curves.....	60
Fig. IV-4. Comparison of measured and calculated neutron-differential-scattering cross sections for the excitation of the first 4+ states of ^{182}W , ^{184}W and ^{186}W . The experimental results are indicated by data symbols and those obtained via calculation by curves.....	61
Fig. IV-5. Illustrative comparisons of measured and calculated differential-scattering cross sections of ^{182}W . Curves indicate the results of calculation; data points the experimental values defined as follows: \square = elastic scattering, \circ = inelastic excitation of the first 2+ level, and X = inelastic excitation of the first 4+ level. The incident neutron energies in MeV are numerical given in each section of the figure. The dimensionality is cross section in b/sr and scattering angle in lab.-deg....	62
Fig. IV-6. Illustrative comparisons of measured and calculated differential-scattering cross sections of ^{184}W . The notation is identical to that of Fig. IV-5.....	63
Fig. IV-7. Illustrative comparisons of measured and calculated differential-scattering cross sections of ^{186}W . The notation is identical to that of Fig. IV-5.....	64
Fig. IV-8. Comparison of measured and calculated neutron inelastic excitation cross sections of ^{182}W . The data points represent the measured values corresponding to the observed excitation energies noted in keV on the various sections of the figure. The curves indicate the results of calculations as described in the text.....	65
Fig. IV-9. Comparison of measured and calculated neutron inelastic excitation cross sections of ^{184}W . The data points represent measured values corresponding to the observed excitation energies noted in keV on the various sections of the figure. Curves indicate the results of calculations as described in the text.....	66

	<u>Page</u>
<u>Figure Captions, Section IV. (Contd.)</u>	55
Fig. IV-10. Comparison of measured and calculated neutron inelastic excitation cross sections of ^{186}W . The data points represent measured values corresponding to the observed excitation energies noted in keV on the various sections of the figure. Curves indicate the results of calculations as described in the text.....	67
Fig. IV-11. Comparison of measured and calculated (with $\beta_2 = 0.205$) neutron cross sections of ^{182}W . Measured values are indicated by symbols as follows: + = neutron total cross sections, 0 = neutron elastic scattering cross sections, \square = cross sections for the excitation of the first 2+ state, and X = cross sections for the excitation of the first 4+ state. Curves "A" (and unmarked) denote the calculated results. Curve "C" indicates the calculated result obtained with the alternate formulation of the resonance fluctuation and correlation corrections as described in the text. Curve "B" indicates the low-energy experimental neutron total cross sections results derived from Ref. IV-9.....	68
Fig. IV-12. Measured and calculated differential neutron elastic scattering cross sections of ^{182}W at an incident neutron energy of 3.5 MeV. The measured values are indicated by circular symbols. The simple curve is the result of calculations using $\beta_2 = 0.223$ and the curve with "tick" marks results obtained with $\beta_2 = 0.205$	69
Fig. IV-13. The Angular Distributions of 2.5 MeV Neutrons Inelastically Scattered from ^{186}W . The distributions are identified by their mean experimental excitation energies. The label "C" refers to compound-nuclear angular shapes as given by spherical compound-nucleus calculations. The label "C + D" refers to the superposition of compound-nuclear and direct-reaction components as described in the text. (Units: b/sr, lab.-deg.....)	70
Fig. IV-14. The Coupled-Channels-Calculated Direct-Reaction Angular Distributions of 2.5 MeV Neutrons Scattered from ^{186}W . The label "O" refers to the coupling scheme involving only the first three members of the ground state rotational band. The label "A" refers to the coupling scheme of "O" plus the first two members of the gamma-vibrational band. The label "B" refers to the coupling scheme of "A" plus the β -vibrational band head. Part (a) shows angular distributions for the first two members (0^+ , 2^+) of the ground state rotational band, while part (b) indicates those for the first two members (2^+ , 3^+) of the gamma-vibrational band and the beta-vibrational band head (0^+). See text for details. Units: b/sr, lab.-deg.....	71

LIST OF FIGURES (Contd.)

	<u>Page</u>
<u>Figure Captions, Section IV. (Contd.)</u>	55
Fig. IV-15. The Angular Distributions of 1.8, 2.5 and 3.0 MeV Neutrons Scattered from the Gamma-Vibrational Band Head in ^{186}W . The label "C" refers to the angular-distribution shape given by spherical compound-nucleus calculations. The labels "A" and "B" refer to the direct-reaction angular-distribution shapes calculated by the coupled-channels method using coupling schemes A and B as defined in Fig. IV-14. The labels "C + A" and "C + B" identify the sums of compound nuclear and direct-reaction components as described in the text. (Units: b/sr, lab.-deg.).....	72
<u>Figure Captions, Section V.</u>	80
Fig. V-1. Comparison of measured and evaluated neutron total cross sections of ^{182}W , ^{184}W and ^{186}W from 0.1 to 5.0 MeV. The present evaluation is indicated by a heavy curve and the present experimental results by circular data symbols. Averages of previously reported data are indicated by light curves noted as follows: "W" = 20 keV average of Ref. V-1, "M" = 100 keV average of Ref. V-5, and "F" = 100 keV average of Ref. V-6.....	81
Fig. V-2. Comparison of measured and evaluated neutron total cross sections of ^{182}W , ^{184}W and ^{186}W from 5.0 to 15.0 MeV. The present evaluation is indicated by the heavy curve. Averages of reported experimental results are indicated by light curves as follows: "M" = 100 keV average of Ref. V-5 and "F" = 100 keV average of Ref. V-6.....	82
Fig. V-3. Evaluated differential-elastic-scattering cross sections of ^{182}W , ^{184}W and ^{186}W . Cross sections are given in b/sr and scattering angle in lab.-deg.....	83
Fig. V-4. Outline of present evaluations for ^{182}W , ^{184}W and ^{186}W . Curves indicate the evaluated cross sections identified as follows: 1 = total, 2 = elastic, 4 = total inelastic, 102 = capture and 91 = continuum inelastic. The cumulative envelopes of the discrete-inelastic components are shown by curves. Data points indicate measured elastic-scattering values: <1.5 MeV from Ref. V-1, >1.5 MeV from this work.....	84
Fig. V-5. Comparison of components of the present ^{186}W evaluation with those of ENDF/B-V. The heavy curves are from ENDF/B-V and the light ones from the present evaluation. Numbers denote reaction types as follows: 1 = total cross sections, 2 = elastic cross sections, 4 = total inelastic cross sections, and 91 = continuum inelastic cross sections.....	85

LIST OF TABLES

<u>No.</u>	<u>Title</u>	<u>Page</u>
II-1.	Measurement Samples.....	3
III-1A.	Observed Excitation Energies for ^{182}W	11
III-1B.	Observed Excitation Energies for ^{184}W	12
III-1C.	Observed Excitation Energies for ^{186}W	13
IV-1.	Base Tungsten Potential Parameters taken from Ref. IV-7.....	52
IV-2.	Level Structure used in Comparing Observed Neutron Inelastic Excitations with Calculations.....	53
V-1.	Total-cross-section Uncertainty Guidelines.....	79

FAST-NEUTRON INTERACTIONS WITH ^{182}W , ^{184}W and $^{186}\text{W}^{*+}$

by

P. T. Guenther, A. B. Smith and J. F. Whalen
Applied Physics Division
Argonne National Laboratory
9700 South Cass Avenue
Argonne, Illinois 60439 U.S.A.

ABSTRACT

Neutron total cross sections of ^{182}W , ^{184}W and ^{186}W are measured from $\approx 0.3 - 5.0$ MeV at intervals of $\lesssim 50$ keV to accuracies of 1 - 3%. Differential neutron elastic- and inelastic-scattering cross sections of the same three isotopes are measured at scattering angles in the range $20 - 160$ deg. and at incident-neutron energy intervals of ≈ 100 keV from $1.5 - 4.0$ MeV. Approximately thirty scattered-neutron groups are observed for each of the isotopes. Prominent of these are excitations attributed to collective rotational and vibrational bands. The experimental results are interpreted in terms of optical-statistical and coupled-channels models with particular attention to the direct excitation of ground-state-rotational and β - and γ -vibrational bands. The strengths of the direct interactions and the magnitudes of the collective deformations are inferred from the interpretations and compared with similar values previously reported elsewhere. The experimental results are used to deduce experimentally-based evaluated data sets for ^{182}W , ^{184}W and ^{186}W over the energy range $0.1 - \approx 5.0$ MeV.

Keywords: Nuclear Reactions: Measured $\sigma_n(\text{total})$ of ^{182}W , ^{184}W , ^{186}W , $0.3 - 5.0$ MeV; Measured $d\sigma/d\Omega_n$ (elastic and inelastic) $1.5 - 4.0$ MeV, $20 - 160$ deg.; Optical-statistical and coupled-channels model interpretations.

*This work supported by the U. S. Department of Energy.

+All measured data reported herein have been transmitted to the National Nuclear Data Center, Brookhaven National Laboratory.

I. INTRODUCTION

The fast-neutron interaction with the even isotopes of tungsten is of basic and applied interest. Approximately 85% of the element consists of the isotopes ^{182}W , ^{184}W , and ^{186}W . These isotopes lie at the upper extreme of a region of static deformation where the degree of deformation is expected to change significantly in four mass units (I-1). Thus, these isotopes offer an unusual opportunity to study the effects of changing deformation on the neutron interaction at few-MeV neutron energies. Such interactions at these energies are a mixture of compound-nucleus and direct-reaction processes not easily studied using charged-particle probes. Neutron excitation of collective rotational and/or vibrational states can be large (I-2), and anomalous excitation of the ground-state rotational band in the complimentary region of changing deformation near $A=150$ has been reported (I-3). It has been suggested that collective excitations are charge dependent (I-4), a postulate that can be examined by comparing parameters deduced from neutron measurements with those reported from charge-sensitive studies (e.g., from proton scattering and coulomb excitation measurements). It has been suggested that neutron total cross sections in this region are sensitive to the character of the deformation (I-5) and observed neutron total cross sections have been interpreted in terms of quadrupole and hexadecupole deformations (I-6). Neutron differential-elastic-scattering distributions are also sensitive to deformation, particularly at large scattering angles (I-7) and the direct-neutron excitation of the ground-state rotational band can be much larger than the compound-nucleus contribution in the several MeV region (I-8).

Elemental tungsten is employed in high-temperature nuclear-energy systems. Some nuclear properties of the even isotopes of tungsten are similar to those of a number of nuclides in the fission-product and actinide regions (e.g., to even rare-earth, uranium, and plutonium isotopes) which are of considerable applied importance but very difficult to experimentally study. Because of these experimental difficulties recourse is often made to theoretical models. The validity of such models is ultimately based upon experimental observation and the present experimental studies of the even isotopes of tungsten provide such a foundation.

The goal of the present work was an improved knowledge of the experimental and calculational understanding of the fast-neutron interaction with the even isotopes of tungsten in the few-MeV region. The experimental methods are outlined in Section II. Section III presents the experimental results and Section IV deals with their interpretation in the context of optical-statistical and coupled-channels models. Section V presents a limited experimentally-based evaluation of the cross sections dealt with in the present study.

References, Section I.

- I.1. Table of Isotopes, 7th Edition, Eds. C. M. Lederer and V. S. Shirley, John Wiley and Sons, Inc., New York (1978).
- I.2. D. Chase, L. Willets and A. Edmonds, Phys. Rev., 110, 1080(1978).
- I.3. D. Coope, S. Tripathi, M. Schell, J. Weil and M. McEllistrem, Phys. Rev., C16, 2223(1977).
- I.4. V. Madsen, V. Brown, S. Grimes, C. Poppe, J. Anderson, J. Davis and C. Wong, Phys. Rev., C13, 548(1976).
- I.5. R. Shamu, E. Bernstein, D. Blondin, J. Ramirez and G. Rochau, Phys. Lett., 45B, 241(1973).
- I.6. Ch. Lagrange, National Soviet Conf. on Neutron Physics, Kiev (1975).
- I.7. P. Guenther, "Elastic and Inelastic Neutron Scattering from the Even Isotopes of Tungsten," Univ. of Ill. Thesis (1977).
- I.8. P. Guenther, D. Havel and A. Smith, "Fast-neutron Excitation of the Ground-state Rotational Band of ^{238}U ," Argonne Natl. Lab. Report, ANL/NDM-16, (1975).

II. EXPERIMENTAL METHODS

A. Samples

The present measurements employed the three isotopically-enriched tungsten samples defined in Table II-1. The samples were fabricated into right-circular cylinders of metallic tungsten using powdered-metallurgical procedures at Oak Ridge National Laboratory (II-1). The sample densities approached that of the elemental metal. Chemical impurities were negligible. It was assumed that the samples were of uniform density although this assumption could not be verified by destructive assay. The similarity of the respective cross sections of the prominent isotopes and the high enrichments of the samples resulted in corrections for minor-isotope content generally much smaller than the experimental uncertainties and thus such corrections were ignored. All cross sections reported herein are stated in terms of "effective atom" of the respective sample. The measurement procedures involved reference-standard samples of hydrogen (polyethylene) and verification samples of elemental carbon all of which were fabricated to the same dimensions as the isotopic tungsten samples. Some ancillary measurements employed elemental tungsten and the requisite samples were machined from high-chemical-purity elemental bar stock.

Table II-1. Measurement Samples

Identification	^{182}W	^{184}W	^{186}W
Weight (gm)	125.7	125.9	124.9
Radius (cm)	1.048	1.041	1.038
Height (cm)	1.996	1.994	1.989

Isotopic Abundance^a in Atom-percent

^{180}W	<0.05	<0.05	<0.05
^{182}W	94.9	1.38	0.58
^{183}W	1.58	1.84	0.41
^{184}W	2.39	98.88	1.34
^{186}W	1.17	2.89	97.66

^aValues provided by Oak Ridge National Laboratory assay.

B. Neutron Total-cross-section Measurements

The neutron total-cross-section measurements were made using the mono-energetic-pulsed-beam facility at the Argonne Fast Neutron Generator. This facility and its application to total-cross-section measurements have been described elsewhere, therefore only an outline is given here (II-2).

The ${}^7\text{Li}(p,n){}^7\text{Be}$ reaction was used as a neutron source with the source dimensions confined to a ≈ 3 mm diameter spot (II-3). The proton beam was pulsed at a 2 MHz repetition rate with a pulse duration of ≈ 1 nsec. The mean neutron energy was determined to within ≈ 10 keV by control of the proton energy and verified by the observation of well known resonances in a number of materials (e.g., carbon) (II-4,5). The neutron source was surrounded by a massive shield with a 1 cm diameter collimating aperture at a zero-degree source-reaction angle. The collimated beam was incident on the transmission samples placed ≈ 25 cm from the collimator exit. The samples were mounted upon a wheel with neutrons incident upon the sample-cylinder bases. The wheel concurrently contained a number of measurement samples, a carbon reference sample and one or more void positions and was rotated in a stepping motion so as to change the sample (or void) positions twenty or more times a minute. No independent monitoring of source intensity was required. A proton-recoil-scintillation detector was placed 4-7 m from the transmission samples on the neutron beam axis. The response of the detector was determined in such a manner as to obtain the time-of-flight of the neutrons from the source, through the sample position, to the detector. The resulting velocity spectra were stored in a digital computer in correlation with the sample-void positions of the sample wheel. The neutron velocity resolution was sufficient to resolve the primary neutron group of the source reaction from the secondary-source group and from the time uncorrelated background and to define the spectral distribution of the neutron beam to within ≈ 100 keV.

The "observed" neutron total cross sections were calculated from the measured sample transmissions in the conventional manner (II-6). In-scattering corrections were estimated, found small, and neglected. Small dead-time corrections were made using a reference-clock pulse introduced into the data-acquisition system. Throughout the tungsten sample measurements the neutron total cross sections of elemental carbon were concurrently determined with good agreement with the values reported in the literature (II-7).

C. Neutron Scattering Measurements

The neutron scattering measurements employed the pulsed-beam fast-neutron time-of-flight technique and the multi-angle detection system at the Argonne Fast Neutron Generator. This measurement apparatus and its application have been extensively described elsewhere and thus the procedures are only outlined here (II-8,9).

The neutron source was again the ${}^7\text{Li}(p,n){}^7\text{Be}$ reaction with the metallic lithium film adjusted to provide incident-neutron energy spreads at the scattering samples of ≈ 10 to 50 keV (II-3). The average energy of the incident neutrons was determined to within ≈ 10 to 20 keV by control of the incident-proton beam. The source was pulsed at a repetition rate of 1 or 2 MHz with a burst duration of ≈ 1 nsec. The scattering samples were placed ≈ 13 cm from the source at a zero-degree source-reaction angle with the neutrons incident upon the cylindrical surfaces of the samples. The scattering samples placed at the common focus of the flight paths. Massive shielding defined the flight paths and protected the detectors from the primary neutron source and various other background components. Most of the measurements were made at scattered-neutron flight paths of ≈ 5.4 m. A few measurements improved the scattered-neutron velocity resolutions by using flight paths of ≈ 20 m. The relative angular placement of the flight paths was determined to within ± 0.5 degrees using optical methods. The absolute setting of the relative angular system was then determined to within ≤ 1.0 degree by the observation, at a fixed incident energy, of the energies of neutrons scattered from hydrogen at a number of angles to both sides of the zero-degree center line.

The neutron detectors consisted of proton-recoil scintillators 13 cm in diameter and 2 cm thick (for measurements at ≈ 5 m flight paths) or 20 cm in diameter and 3 cm thick (for measurements at ≈ 20 m flight paths). Pulse-shape-sensitive circuitry was employed to suppress gamma-ray-induced backgrounds in the detectors. An additional time-of-flight system, supported by an array of long counters, monitored the primary source intensity (II-10). The monitors were arranged so as to be insensitive to the physical placement of the flight-path collimators. The relative energy-dependent response of each of the detectors was determined by observation of the neutrons emitted at the spontaneous fission of ${}^{252}\text{Cf}$ and/or by the observation of neutrons scattered from hydrogen over a range of scattering angles (II-11). The absolute normalizations of these relative responses were determined by the observation of neutrons scattered from hydrogen at each of the measurement energies. The responses of the ten detectors were determined in a largely independent manner thus there was a considerable degree of redundancy in the determination of cross section magnitudes. These calibration and measurement procedures imply that the tungsten scattering cross sections were measured relative to the well known $\text{H}(n,n)$ cross sections (II-12). Throughout the scattering measurements the fidelity of the measurement system was verified by the concurrent measurement of the well known $\text{C}(n,n)$ cross sections (II-7).

The eleven measured velocity spectra (ten scattering channels and a monitor channel) and associated detector proton-recoil responses were stored in a digital computer system. Subsequent off-line analysis reduced the observed spectra to neutron cross sections in a manner described in Ref. II-9. All of the cross section results, including those associated with the hydrogen reference standard, were corrected for angular-resolution, beam-attenuation, and multiple-event effects using a combination of Monte-Carlo and analytical procedures as described in Ref. II-9.

References, Section II.

- II-1. The authors are indebted to Mr. E. Kobisk et al., Oak Ridge National Laboratory, for the fabrication of the tungsten samples.
- II-2. A. Smith and J. Whalen, "Comments on Energy-Averaged Neutron Total Cross Sections," Argonne National Laboratory Report, ANL/NDM-33 (1977).
- II-3. J. Meadows and D. Smith, "Neutrons from Proton Bombardment of Natural Lithium," Argonne National Laboratory Report, ANL-7938 (1978).
- II-4. G. D. James, Proc. Sym. on Neut. Stds. and Applications, National Bureau of Standards Pub., NBS-SP-493 (1977).
- II-5. S. Cierjacks, P. Forti, D. Kopsch, L. Kropp, J. Nebe and H. Unfeld, "High Resolution Total Neutron Cross Sections between 0.5-3.00 MeV," Karlsruhe Report, KFK-1000 (1968).
- II-6. D. Miller, "Fast Neutron Physics," Vol.-II, Eds. J. Marion and J. Fowler, Interscience Pub., N.Y. (1963).
- II-7. A. Smith, R. Holt and J. Whalen, "Neutron Scattering from ^{12}C in the Few MeV Region," Argonne National Laboratory Report, ANL/NDM-43 (1978).
- II-8. A. Smith, P. Guenther, R. Larson, C. Nelson, P. Walker and J. Whalen, Nucl. Insts. and Methods, 50, 277(1967); see also P. Guenther, A. Smith and J. Whalen, Phys. Rev., C12, 1797(1975).
- II-9. P. Guenther, "Elastic and Inelastic Neutron Scattering from the Even Isotopes of Tungsten," Univ. of Illinois Thesis (1977).
- II-10. A. Hanson and J. McKibben, Phys. Rev., 72, 673(1947).
- II-11. A. Smith, P. Guenther, R. Sjoblom, Nucl. Instr. and Methods, 140, 397(1977).
- II-12. J. Hopkins and G. Breit, Nucl. Data, A9, 137(1971).

III. EXPERIMENTAL RESULTS

A. Neutron Total Cross Sections

The objective was energy-averaged neutron total cross sections comparable with the differential-scattering results and the predictions of energy-averaged models. Therefore the experimental resolutions were chosen to be ≈ 20 -50 keV and generally averaged fluctuating structure excepting, possibly, at the very lowest energies of the present measurements. The measurements were made during three different periods in each of which the cross sections were determined from a few-100 keV to 5 MeV in steps of $\lesssim 50$ keV. The results of the three sets of measurements were generally consistent to within the 1-3% statistical accuracies of the individual measurements. It was believed that systematic experimental uncertainties were generally smaller than the statistical uncertainties.

The above "observed" cross sections are strictly relevant only to the specific samples employed in the measurements. It has been shown by Poenitz et al. (III-1) that self-shielding perturbations can be significant in broad-resolution neutron-total-cross-section measurements involving heavy nuclides in the few-100 keV region. The "observed" value can be considerably smaller than the "true" or infinitely-thin-sample value. The correction of the "observed value" for self-shielding can be calculated from the statistical properties of the underlying fluctuating structure, as described in Ref. III-1, or determined experimentally using a wide range of transmission-sample thicknesses. The latter approach was not explicitly possible in the present case as the integrity of rare samples could not be destroyed. Therefore, the calculational procedures of Ref. III-1 were followed. The potential cross sections and average resonance properties were derived from optical-model phase shifts using an optical potential that described the low energy behavior of the observed neutron total cross sections. Assuming a single-level Breit-Wigner resonance formulation, average level spacings from a fermi gas model and Wigner and Porter-Thomas distributions of level-spacings and width-fluctuations, respectively, a monte-carlo simulation of the resonance cross sections was constructed from which the correction factors applicable to the present experiments were inferred. The details of the calculational procedure are contained in Ref. III-1. The resulting correction factors can be large at low energies as illustrated in Fig. III-1A where, for the present samples, the effect is nearly 20% at 100 keV; decreasing with energy to a negligible effect at 1 MeV.

It is possible to experimentally test the above calculated correction factors in an elemental context. Assuming the element consists of only the present three isotopes ($\approx 85\%$ abundance), corrections applicable to elemental measurements can be derived from the above isotopic correction factors. These elemental correction factors were applied to the results of elemental neutron-total-cross-section measurements made with a wide range of sample thicknesses and incident energies with the results illustrated in Fig. III-1B. The elemental cross-section results obtained with a wide range of sample thicknesses, when corrected with the above deduced factors, are constant with sample thickness to well within their respective statistical accuracies and to generally better than 1%. This experimental test gives confidence in the correction factors that were applied to all of the present

isotopic neutron-total-cross-section results. Similar corrections were made to the low-energy results previously obtained at this laboratory as the identical samples were involved (III-2).

The three sets of corrected data from the present measurements were combined and averaged over 50 keV intervals to 2.0 MeV and over 100 keV intervals at higher energies. The uncertainties in the averaged quantities were defined as the RMS values of the statistical uncertainties of the individual components making up the respective average quantity. These average results are illustrated in Fig. III-2. Qualitatively, the neutron total cross sections of these three isotopes are very similar. However, there are magnitude differences, particularly in the energy range $\approx 0.3 - 2.0$ MeV where the total cross sections of ^{184}W and ^{186}W are nearly identical while those of ^{182}W are systematically smaller. There are also energy-dependent shape differences that cannot be attributed to erroneous sample densities. The possible physical implications of these differences are discussed in Sec. IV, below.

There are only three sets of previously reported data that are directly comparable with the present results. Whalen et al. (III-2) have reported neutron-total-cross-section results for all three isotopes from 0.1 to 0.65 MeV. As corrected (see above), the results of Ref. III-2 are in very good agreement with those of the present work. They do display more fluctuating structure due to their finer resolution. Martin et al. (III-3) have reported neutron total cross sections for the three isotopes from $\approx 0.7 - 15$ MeV. The ^{184}W and ^{186}W results of Ref. III-3 are not qualitatively consistent with those of the present work in either shape or magnitude (as illustrated in Fig. III-2) with the lower-energy region deviating by 10% or more from the present results and from an extrapolation of the values of Ref. III-2. The differences are energy dependent and not simply attributable to sample-density effects or to the above self-shielding phenomena. Foster and Glasgow (III-4) have reported neutron total cross sections of the present three isotopes over the energy range 2.5 - 15.0 MeV. Their results are generally consistent with those of the present work as illustrated in Fig. III-2. The isotopes of the present study make up $\approx 85\%$ of the element. Thus, assuming the neutron total cross sections of the remaining $\approx 15\%$ of the isotopes are similar to those of the even isotopes measured here, the weighted average of the present results should agree with the neutron total cross sections reported for the natural element (III-5). An inspection of the available information indicates that is true within the respective experimental uncertainties.

B. Elastic Neutron Scattering

The primary elastic-scattering-measurement problem was the experimental resolution of the elastic-neutron group from the inelastic neutron component corresponding to the excitation of the first level at ≈ 110 keV. Most of the measurements were made with flight paths of ≈ 5 m and resolved the elastic component to energies of ≈ 2.5 MeV as illustrated by the time distribution of Fig. III-3. At higher incident energies and forward scattering angles the resolution was less complete therefore selected measurements were made at flight paths of ≈ 20 m. With these longer flight paths the resolution improved as illustrated in Fig. III-4. However, the ≈ 20 m flight-path measurements were tedious and thus undertaken only at selected energies (e.g. 2.5, 3.0

and 3.5 MeV) and the results used to correct lesser-resolution ≈ 5 m flight-path results obtained at nearby incident energies for the partially resolved inelastic-neutron contaminant.

Measurements were generally made at intervals of ≈ 200 keV from 1.5 to 4.0 MeV with incident-neutron resolutions of $\lesssim 20$ keV and at $\gtrsim 20$ scattering angles distributed between 20-160 deg. At some incident energies a large number of distributions were obtained over a period of time (e.g. at 3.0 MeV), cumulatively amounting to more than 100 differential cross section values, each with essentially independent normalizations. In these highly redundant cases the data were averaged to obtain distributions consisting of 20-30 differential values. The resulting differential-elastic-scattering cross sections are summarized in Figs. III-5A, B and C. The quality of these distributions varies depending upon the statistical accuracies of the particular measurements, the care taken with the detector normalizations, the experimental resolutions employed in the particular measurements and the number of independent components of a given distribution. Generally, the statistical accuracies of the differential measurements were several percent and frequently $\approx 1\%$. The detector normalizations were reproducible to 3-5%. Correction procedures, e.g. those correcting for multiple events, generally introduced an additional 1-5% uncertainty except near the extreme cross-section minima where uncertainties due to the correction factors could become larger. Uncertainties associated with the knowledge of the H(n,n) reference cross section were relatively small (i.e. $\lesssim 1.0\%$). A primary concern in estimating uncertainties was the effect of varying experimental resolutions. In some cases the resolution was relatively good and its influence could be quantitatively determined as illustrated by the gaussian fitting of the time distribution of Fig. III-3. In other cases the estimate of the effect of resolution was far more subjective but was made with a conservative philosophy. These various factors contributing to the uncertainties associated with the differential-elastic-scattering data are reflected by the error bars indicated in the three portions of Fig. III-5.

The measured differential-elastic-scattering cross sections were least-square fitted with a Legendre-polynomial series of the form

$$\frac{d\sigma}{d\Omega} = \frac{\sigma}{4\pi} \left[1 + \sum_{\ell=1}^8 \omega_{\ell} P_{\ell} \right] \quad (\text{III-1})$$

where ω_{ℓ} and P_{ℓ} are conventional omega coefficients and Legendre polynomials, respectively. The fitting procedure was constrained to be consistent with Wick's Limit (III-6) at zero degrees and to provide a relatively smooth energy dependence of the extrapolation to 180 deg. cross-section values. The results of these fitting procedures are illustrated in Figs. III-5 and 7. Generally, the behavior of the distributions derived from the fitting follows a smooth-energy dependence with the largest deviations confined to those cases where only a limited number of experimental values were available. The fitting procedures also provided the angle-integrated elastic scattering cross sections shown in Fig. III-6. The

estimated uncertainties in these angle-integrated cross sections varied from 5 to 7% and the individual results were consistent to well within this estimate.

Previously reported elastic measurements of neutron scattering from these isotopes of tungsten appear to be confined to the lower energy work of Lister et al. (III-7) and the 3.4 MeV results of Delaroche et al. (III-8). The present results reasonably extrapolate to the lower-energy values of Lister et al. as illustrated in Fig. III-6. The present 3.5 MeV results generally agree with those reported by Delaroche et al. to within the respective experimental uncertainties as illustrated in Fig. III-7.

C. Neutron Inelastic Scattering

The majority of the neutron-inelastic-scattering measurements were made with ≈ 5 m flight paths distributed over the angular range 20-160 deg. Some additional measurements employed ≈ 20 m flight paths in order to improve the resolution of the elastic component from the nearby inelastic contributions as illustrated in Fig. III-4. There were a number of experimental results with varying detector angles, detector sensitivities and scattered-neutron resolutions. The definition of a given inelastic-neutron group was optimum over a limited energy range and sensitive to the particular instrument configuration. Therefore the measurements were made in systematic incident-energy steps so that the inelastic-neutron groups identified in regions of optimum definition could be followed into regions of marginal resolution. This approach is illustrated in Fig. III-8. Where at all possible, artifacts due to multiple-events and/or to contributions from the second neutron-group from the source reaction were identified and removed. Such corrections introduced some additional uncertainties in both the excitation energies and the corresponding cross sections.

The observed inelastic-neutron excitation energies were determined from the velocity spectra using the measured flight times, incident energies and flight paths. The energy scales were verified by the observation of well known inelastic-neutron groups (e.g. that resulting from the excitation of the 846 keV state in ^{56}Fe). A neutron group was accepted for the excitation-energy determination only if observed with reasonable reliability on at least five occasions each involving several independent detectors. Some of the prominent inelastic-neutron groups were clearly observed more than 100 times. The "observed" excitation energy was defined as the simple average of the individual measured values with the uncertainty expressed as the RMS deviation from the mean. In this manner approximately 30 scattered-neutron groups were identified for each of the three isotopes as summarized in Table III-1A, B and C. Many of these correspond to excitation energies of ≥ 1.5 MeV where the experimental resolution was not comparable to the detail of the expected structure. Even at excitation energies of < 1.5 MeV it was apparent that many of the observed levels were composites of contributions from a number of true levels generally closer-spaced than the experimental resolution. Qualitative plots of observed level density versus excitation energy behaved in the expected approximately exponential

Table III-1A. Observed Excitation Energies for $^{182}\text{W}^a$

No.	E_x (keV)	No.	E_x (keV)
1	102 ± 8	19	2059 ± 25
2	326 ± 15	20	2121
3	671 ± 14	21	2185
4	1138 ± 16	22	2247
5	1229 ± 12	23	2299
6	1281 ± 22	24	2382 ± 28
7	1309 ± 18	25	2468 ± 15
8	1357 ± 21	26	2543 ± 22
9	1428 ± 38	27	2615 ± 15
10	1492 ± 15	28	2690
11	1539 ± 16	29	2768
12	1618 ± 24	30	(2819)
13	(1678)	31	(2867)
14	1745 ± 23	32	(2932)
15	1792 ± 20	33	(2979)
16	1858 ± 20	34	(3022)
17	1914 ± 20	35	(3062)
18	1988 ± 21		

^aUncertainties are RMS values determined from at least four measurements. Parenthesis indicate tentative assignments of observed quantities often due to the excitation of several levels. No uncertainty is given if less than five observations were available.

Table III-1B. Observed Excitation Energies for ^{184}W

No.	E_x (keV)	No.	E_x (keV)
1	111 ± 10	16	1911 ± 25
2	365 ± 20	17	2008 ± 30
3	737 ± 32	18	2105 ± 37
4	905 ± 24	19	2155 ± 34
5	1000 ± 24	20	2240 ± 25
6	1125 ± 17	21	2324 ± 24
7	1237 ± 31	22	2440
8	1323 ± 43	23	2520
9	1376 ± 23	24	2580
10	1435 ± 17	25	2638
11	1528 ± 12	26	2663
12	1613 ± 18	27	2735
13	1667 ± 13	28	(2811)
14	1725 ± 29	29	(2866)
15	1787 ± 32	30	(2918)

Table III-1C. Observed Excitation Energies for ^{186}W

No.	E_x (keV)	No.	E_x (keV)
1	121 ± 7	19	2004 ± 15
2	399 ± 10	20	2073 ± 12
3	742 ± 7	21	2118 ± 12
4	858 ± 18	22	2177 ± 13
5	950 ± 21	23	2241 ± 26
6	1028 ± 32	24	2347 ± 18
7	1182 ± 26	25	2406 ± 12
8	1296 ± 31	26	2462
9	(1397 ± 35)	27	2552
10	1449 ± 24	28	2643
11	1515 ± 35	29	(2713)
12	1589 ± 19	30	(2768)
13	1656 ± 21	31	(2820)
14	(1685 ± 10)	32	(2868)
15	1728 ± 25	33	(2933)
16	1805 ± 15	34	(2979)
17	1893 ± 29	35	(3023)
18	1942 ± 35	36	(3063)

manner to excitation energies of 1.5 - 2.0 MeV then departed from the exponential form as would be expected from incomplete experimental resolutions. Thus, the majority of excitations given in Table III-1 should be interpreted as observables within the context of the experimental resolution. However, the excitation energies are reasonably consistent with previously reported level information as illustrated in Fig. III-9.

The neutron-inelastic-scattering cross sections were derived from the measured velocity spectra in a manner analogous to that employed in the context of elastic scattering. Due to the complexity of the inelastic velocity spectra subjective judgments were involved with consequent increased uncertainties. Differential-inelastic-scattering cross sections were accepted when they were observed at a minimum of three scattering angles and several incident neutron energies. In the case of some of the prominent inelastic-neutron groups several hundred independent differential-cross-section values were available. With the better-resolution-measurements cross sections for several inelastic groups were obtained which corresponded to a single cross-section value observed at a lesser resolution. In such cases the cross section derivation sought the most accurate cross section value rather than the best possible resolution of the components and thus the values for the composite of several contributions was usually emphasized.

At excitation energies ≤ 0.8 MeV neutron inelastic scattering from the present three isotopes is dominated by contributions from the ground-state-rotational band; ≈ 110 keV (2+), ≈ 350 keV (4+) and (to a much less extent) the ≈ 700 keV (6+) states. Angular-distribution anisotropy for the excitation of the first two states (2+, 4+) increased rapidly with energy. A number of measured differential cross section values corresponding to the excitation of the first 2+ and 4+ states were combined and averaged where the angles and energies were very similar to obtain the differential cross section distributions shown in Figs. III-10 and -11. The anisotropy of the distributions is clearly evident in these two figures. Qualitatively, these cross section magnitudes for the three isotopes are similar but there are detailed differences in both shape and magnitude. The angle-integrated inelastic scattering cross sections were determined by least-square fitting Eq. III-1 to the measured differential values with the fitting procedure constrained to provide a reasonably smooth energy-dependence of the 0 and 180 deg. extrapolations. Extreme forward- and backward-angle measured values were often least reliable and their uncertainties could influence the polynomial extrapolations well beyond the measured angular range without some sort of constraint. Above ≈ 3.0 MeV the measured values were more limited in angular scope and usually available at only a few incident energies where the flight path was extended to ≈ 20 m. The angle integrated cross sections resulting from the above fitting procedures are summarized in Figs. III-12A, B and C.

Above ≈ 0.8 MeV excitations the neutron groups become increasingly complex and blend into unresolved groups of states at excitations of ≈ 1.5 MeV. The corresponding differential cross sections generally approach isotropy as illustrated in Fig. III-13. Some small anisotropy was observed for cross sections associated with the excitation of 0+ states and/or the β - and γ -vibrational

bands as discussed below. Again, the differential cross sections were fitted with legendre series to obtain the angle-integrated cross sections summarized in Figs. III-12A, B and C. The fitting procedures always used low-order polynomials (e.g. $\leq P_2$) and often assumed isotropy. At higher excitation energies the neutron-inelastic-scattering cross sections of the three isotopes are noticeably different as one might expect from the level structure of Fig. III-9.

The uncertainties associated with the above differential and angle-integrated inelastic-scattering cross sections varied from an optimum of 5% in the best defined cases to 30-50% (or even more) in the marginally observed cases. The respective uncertainties are shown in Figs. III-12A, B and C. The origin of these uncertainties was similar to that outlined above in the context of elastic scattering with much greater emphasis on subjective judgments. The latter were felt to be conservative. The uncertainty estimates were supported by the reproducibility of the results measured over an extended period of time. In addition, the cumulative sum of the above neutron-inelastic- and elastic-scattering components is generally consistent with the observed neutron total cross section over wide energy ranges as discussed in Sec. V., below.

Apparently, only two previous measurements of neutron-inelastic scattering from the present isotopes have been reported. Lister et al. (III-7) have reported experimental values at energies of <1.5 MeV. Their results very nicely extrapolate to the present values as illustrated in Figs. III-12A, B and C. Delaroche et al. (III-8) have reported measured cross sections for the excitation of the ground-state-rotational band at an incident neutron energy of 3.4 MeV. Their results are compared with the present 3.5 MeV values in Fig. III-14. There is qualitative agreement, largely within the uncertainties of the respective measurements. However, there is some tendency for the magnitudes of the results of Ref. III-8 to be systematically larger than those of the present work. There have been some experimental studies of inelastic-neutron scattering from elemental tungsten but those results cannot be simply related to the present isotopic work.

References, Section III.

- III-1. W. Poenitz, J. Whalen and A. Smith, "Total-Neutron Cross Sections of Heavy Nuclei," accepted for publication in Nucl. Sci. and Eng. (1980).
- III-2. J. F. Whalen et al., Argonne Natl. Lab. Report, ANL-7210 (1966).
- III-3. R. C. Martin, P. F. Yergin, R. H. Augustson, N. N. Kaushal, H. A. Medicus and E. J. Winhold, Bull. Am. Phys. Soc., 12, 106(1967).
- III-4. D. Foster and D. Glasgow, Phys. Rev., C3, 576(1971).
- III-5. Neutron Cross Sections, Brookhaven Natl. Lab. Report, BNL-325, Vol. 2, 3rd Edition, Editors D. Garber and R. Kinsey (1976).
- III-6. See A. Lane and R. Thomas, Rev. Mod. Phys., 30, 257(1958).
- III-7. D. Lister, A. Smith and C. Dunford, Phys. Rev., 162, 1077(1967).
- III-8. J. Delaroche, G. Haouat, R. Shamu, J. Lackhar, M. Patin, J. Sigaud and J. Chardine, Natl. Soviet Conf. on Neutron Phys., Kiev (1977); see also, Conf. on Nucl. Cross Sections for Technology, Natl. Bureau of Standards Pub., NBS-SP-594 (1980).
- III-9. Table of Isotopes, 7th Edition, Eds. C. M. Lederer and V. S. Shirley, Wiley Interscience Pub., New York (1978).

Figure Captions, Section III.

- Fig. III-1A. Neutron-total-cross-section self-shielding correction factors for ^{186}W . Vertical axis gives the correction factor, the horizontal axis the sample thickness in nuclei/barn (n/b). Curves correspond to various neutron energies distributed from 100 to 500 keV. One and two cm sample thicknesses are noted by arrows.
- Fig. III-1B. Relative fully-corrected measured neutron total cross sections of elemental tungsten at illustrative energies of 98, 325 and 475 keV as a function of sample thickness given in nuclei/barn (n/b). Error bars indicate experimental statistical accuracies.
- Fig. III-2. Neutron total cross sections of ^{182}W , ^{184}W and ^{186}W . The present experimental results are indicated by data points. Curves denote averages of previously reported experimental results referenced as follows: A = 10 keV average of Ref. III-2, B = 100 keV average of Ref. III-3, and C = 100 keV average of Ref. III-4.
- Fig. III-3. Neutron time-of-flight spectrum obtained by scattering 1.8 MeV neutrons from ^{186}W at an angle of 115 deg. (Histogram). The flight-path was 5.5 m. The smooth curve indicates the result of fitting two gaussian distributions to the measured values corresponding to the elastic- and inelastic-(observed $E_x = 122$ keV) neutron groups.
- Fig. III-4. Representative ^{186}W time-of-flight spectra obtained at an incident energy of 3.0 MeV with a flight path of ≈ 20 m. Scattering angles are noted on the individual figures. The elastically-scattered neutron group is to the right of each figure, the inelastic group ($E_x \approx 121$ keV) to the left. All distributions are normalized to the same maximum heights. Small ($\approx 5\%$) backgrounds have been subtracted. Maximum events per measurement time vary from several times 10^3 to several times 10^2 .
- Fig. III-5. Measured differential-neutron-elastic-scattering cross sections of ^{182}W (A), ^{184}W (B) and ^{186}W (C). Data points indicate the measured values and curves the results of least-square fitting Eq. III-1 to the measured results as described in the text. (Cross-sections are given in b/sr and scattering angle in lab.-deg.)
- Fig. III-6. Measured neutron elastic-scattering (circular symbols) and total (crosses) cross sections of ^{182}W , ^{184}W and ^{186}W . The elastic scattering values at energies below 1.5 MeV were taken from Ref. III-7. Curves are "eye-guides" described in Sec. V of the text.
- Fig. III-7. Illustrative measured neutron differential-elastic-scattering cross sections of ^{182}W (A), ^{184}W (B) and ^{186}W (C). The present experimental results are noted by circular data points, those of Ref. III-8 by crosses. Curves denote the results of a least-square fit of Eq. III-1 to the present measured values as described in the

Figure Captions, Section III. (Contd.)

text. Incident neutron energies are numerically given in MeV (cross sections are in b/sr and scattering angle in lab.-deg.).

- Fig. III-8. Representative TOF spectra for ^{186}W obtained at several incident energies. Primed quantities indicate scattering from the second source-reaction group. Incident energies (MeV) and specific observed excitation energies (keV) are numerically noted. Plural scattering is also indicated. The inelastic neutron groups are emphasized with gaussian eye-guides. The gradual loss of resolution, as well as the increased complexity of the spectra, with incident energy is evident.
- Fig. III-9. Excitations observed in the present neutron-scattering experiments (boxes) compared with the level structure given in the compilation of Ref. III-9. Reported excitation energies in MeV and J^π values are given to excitations of ≈ 1.2 MeV. More details of the structure information are given in Ref. III-9.
- Fig. III-10. Angular distributions of neutrons resulting from the excitation of the $2+$ member of the ground-state rotational band of ^{182}W , ^{184}W and ^{186}W . Measured values are indicated by data points. Curves denote the results of a least-square fit of Eq. III-1 to the measured values. Scattering angle is given in lab.-deg. and cross section in b/sr.
- Fig. III-11. Angular distributions of neutrons resulting from the excitation of the $4+$ member of the ground-state rotational band of ^{182}W , ^{184}W and ^{186}W . Notation is identical to that of Fig. III-10.
- Fig. III-12. Inelastic-neutron-scattering excitation cross sections of; (A) ^{182}W , (B) ^{184}W , and (C) ^{186}W . Circular data points indicate measured values where those at energies of less than 1.5 MeV are taken from Ref. III-7. Crossed data points indicate measured results combined with the previous (and lower energy) excitation. Observed excitation energies are numerically given in keV. Curves are "eye-guides" constructed through the measured values.
- Fig. III-13. Some illustrative differential-neutron-scattering cross sections of the ^{186}W at an incident neutron energy of 3.0 MeV. Data points indicate measured values with excitations given in keV. Curves are the results of least square fitting procedures as described in the text. Scattering angle is given in lab-degrees and cross section in b/sr.
- Fig. III-14. Comparison of measured cross sections for the excitation of the $2+$ and $4+$ states of the ground-state rotational bands of ^{182}W , ^{184}W and ^{186}W . Circular data points indicate the results of the present work at an incident energy of 3.5 MeV, crosses the results of Delaroche et al. (III-9) at an energy of 3.4 MeV. Cross section is given in b/sr and scattering angle in lab-deg.

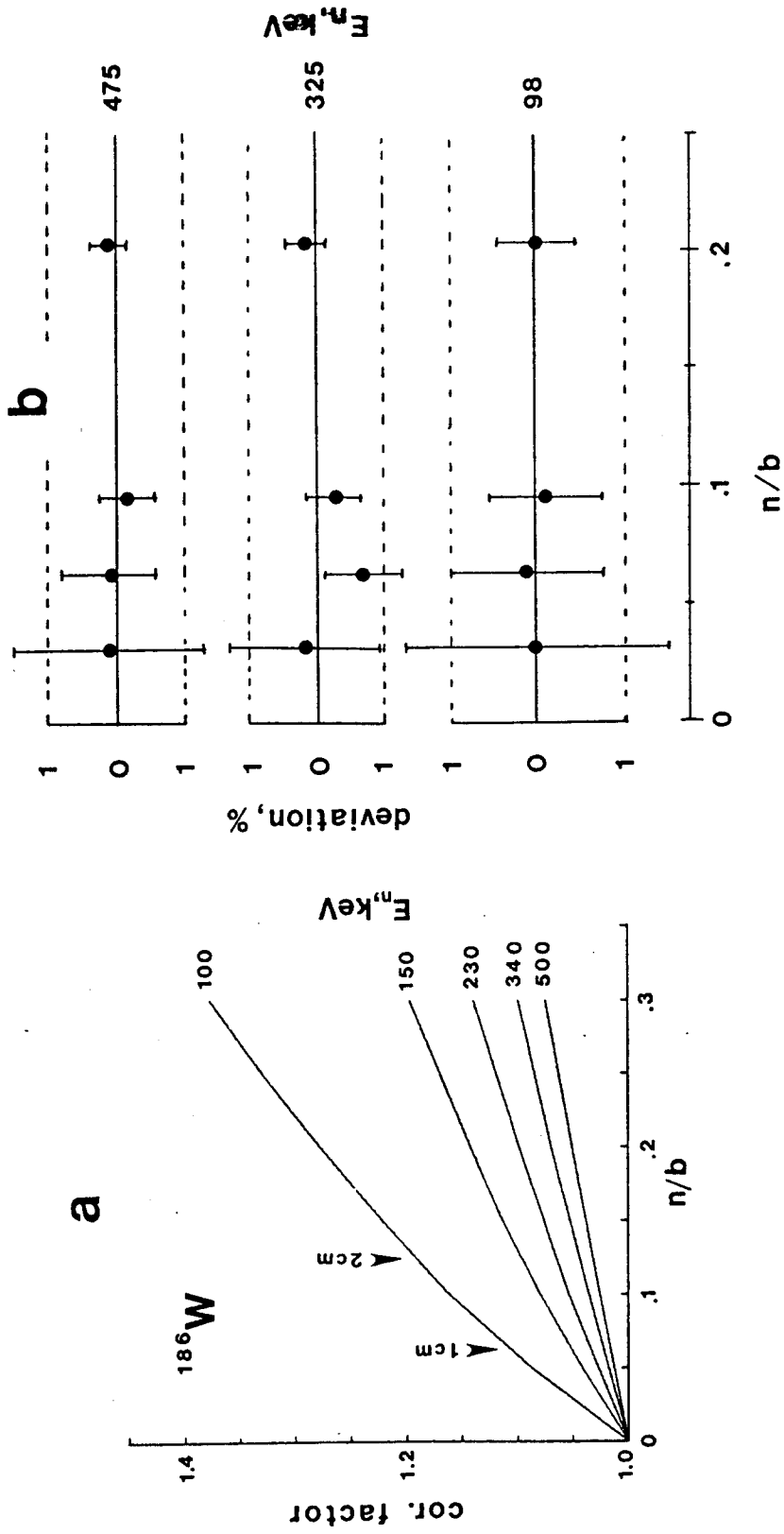


Fig. III-1.

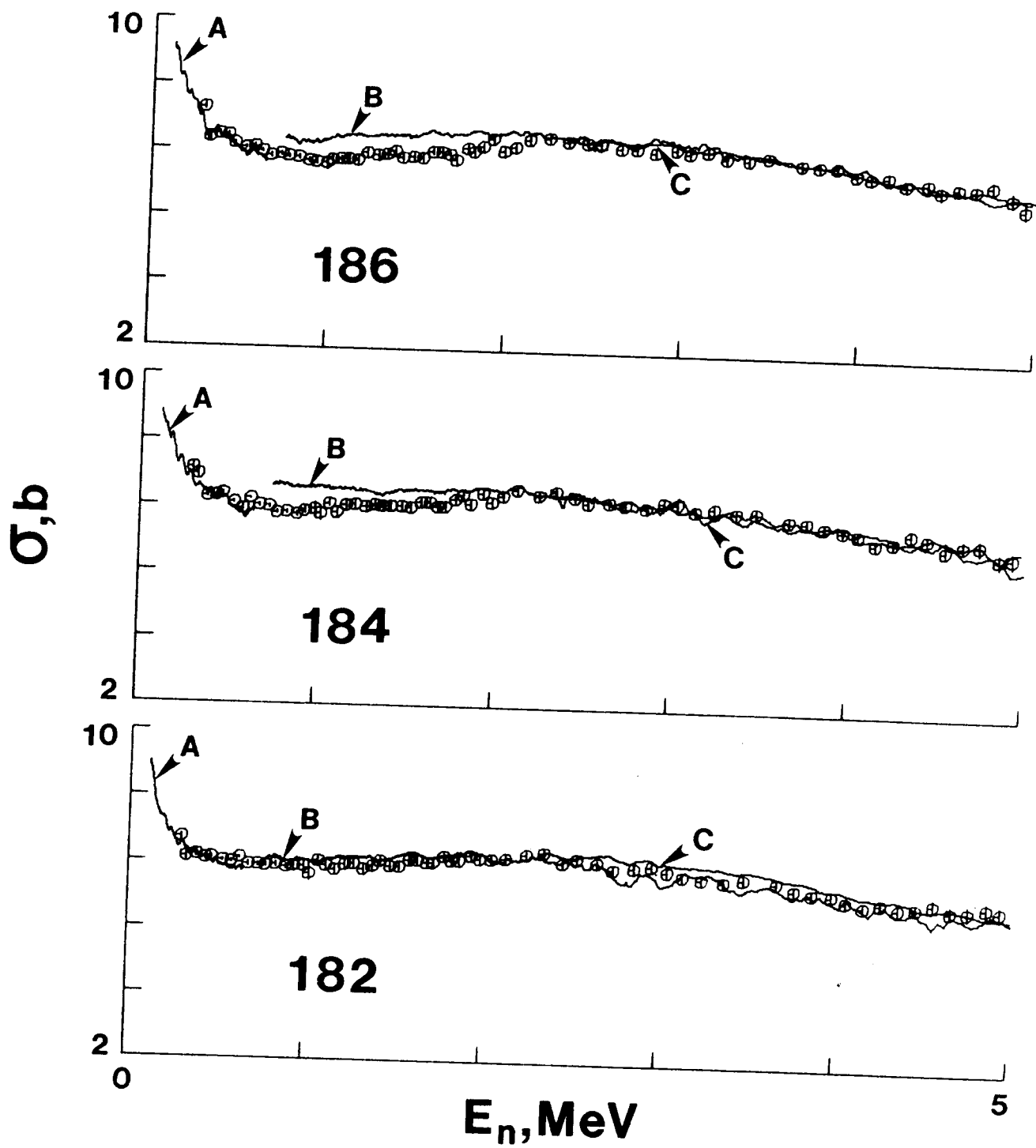


Fig. III-2.

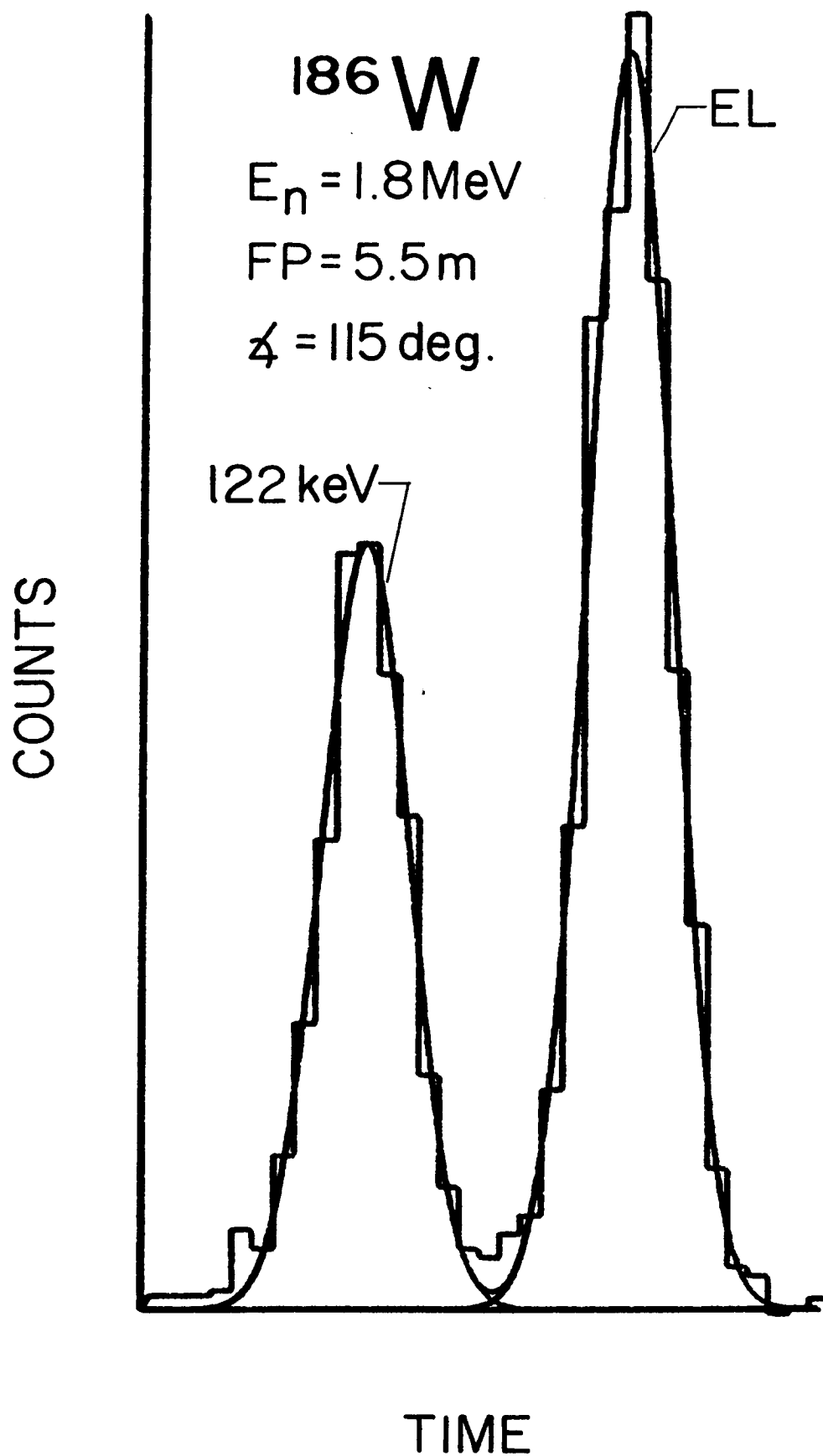


Fig. III-3.

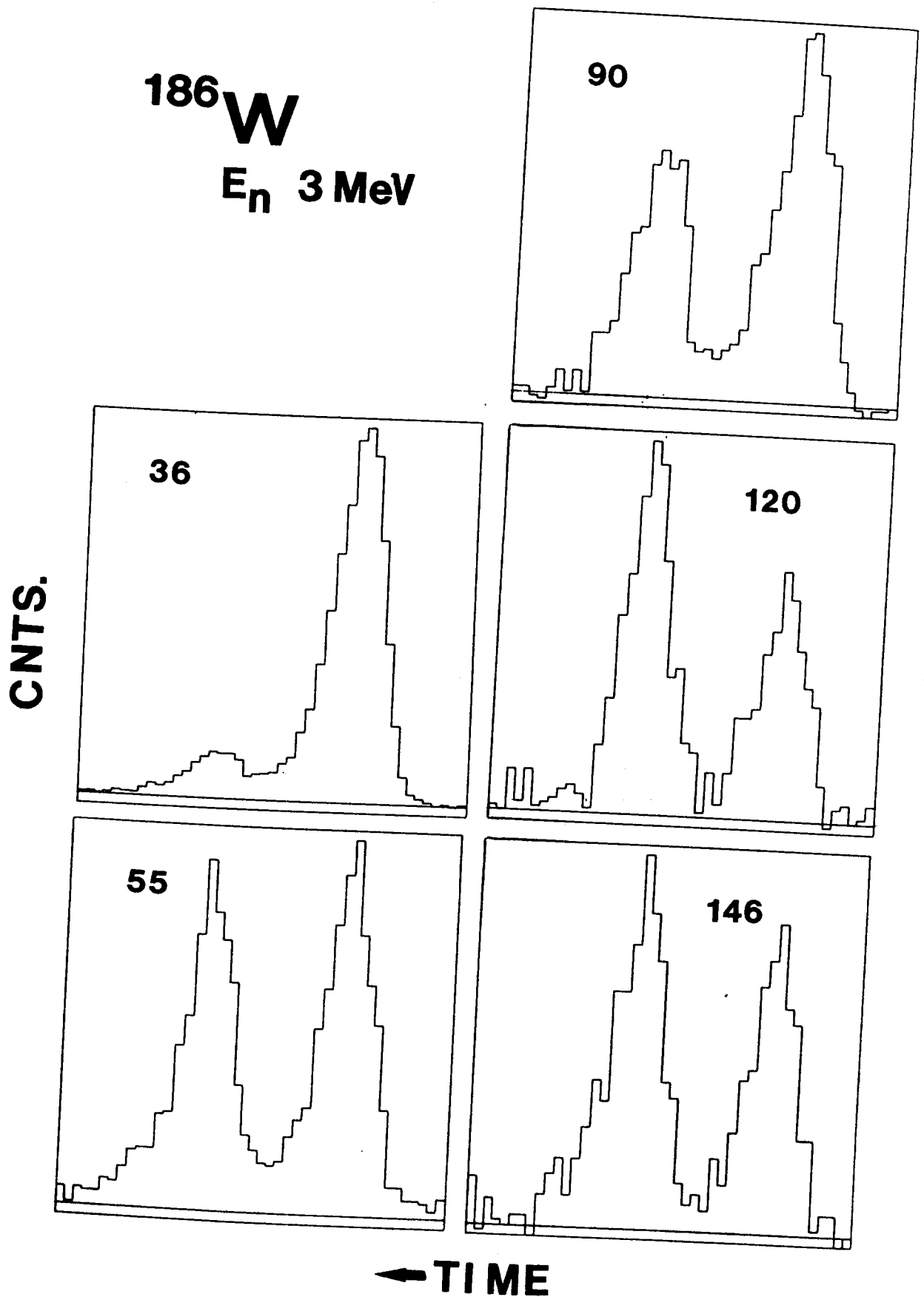


Fig. III-4.

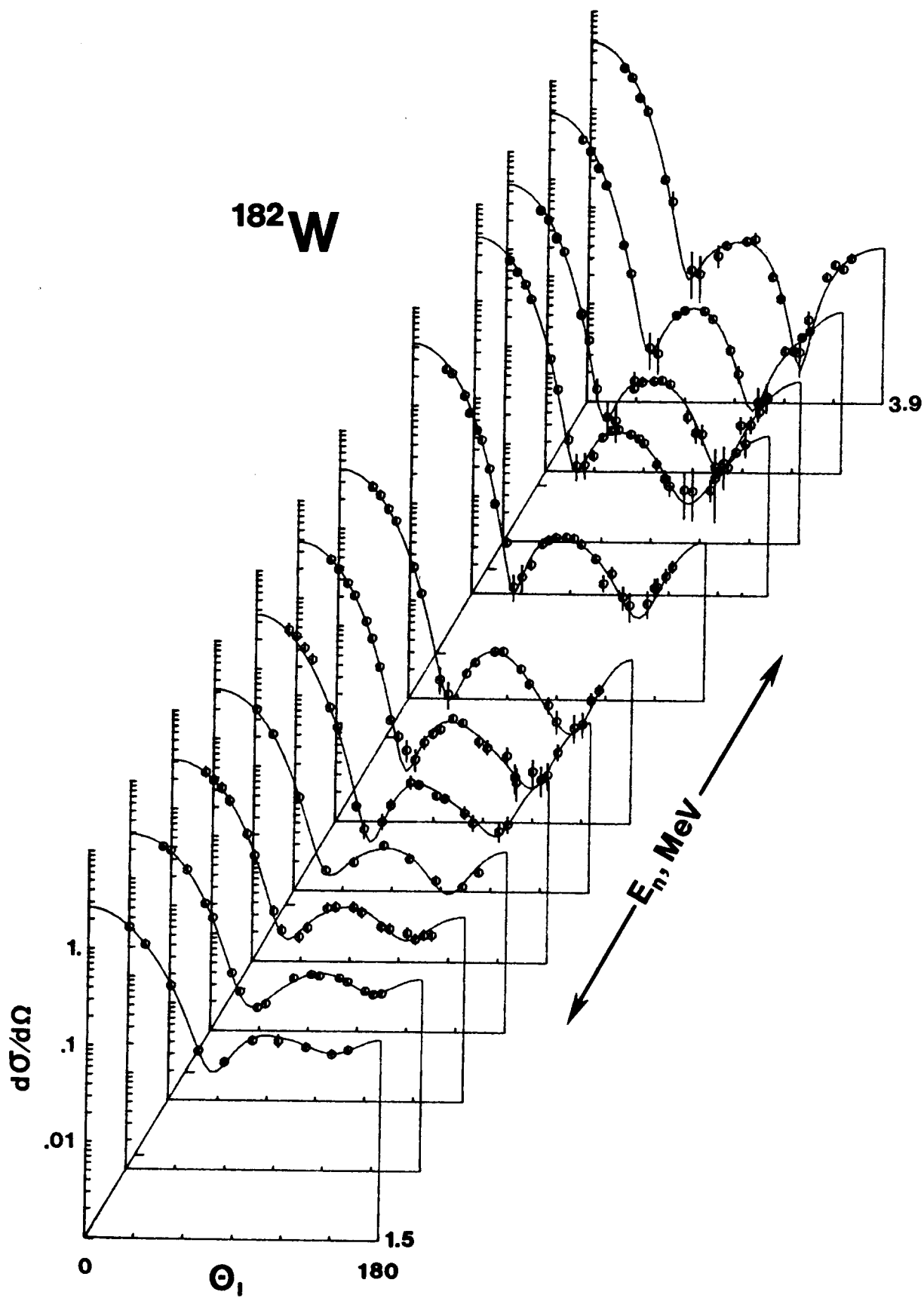


Fig. III-5A.

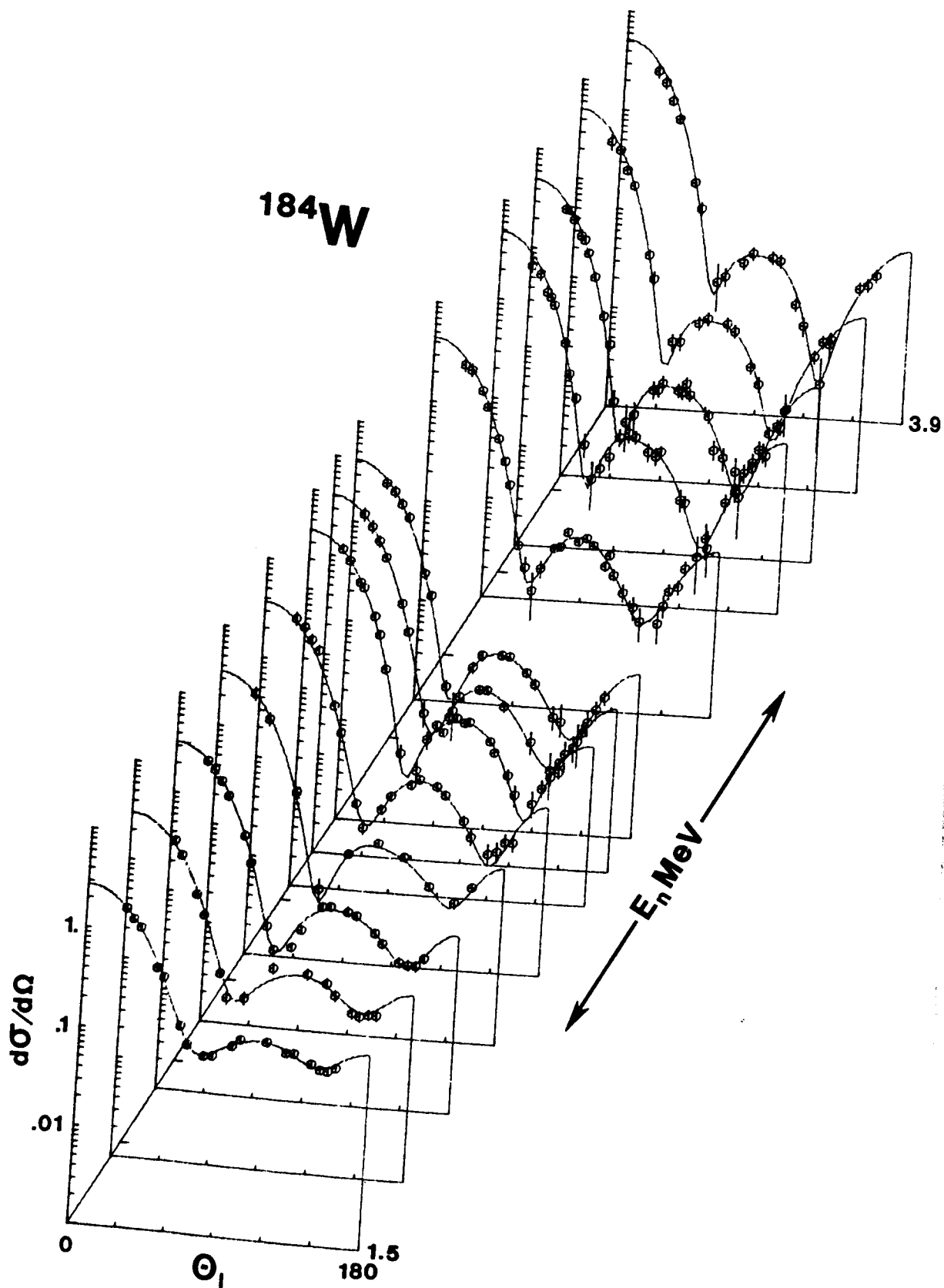


Fig. III-5B.

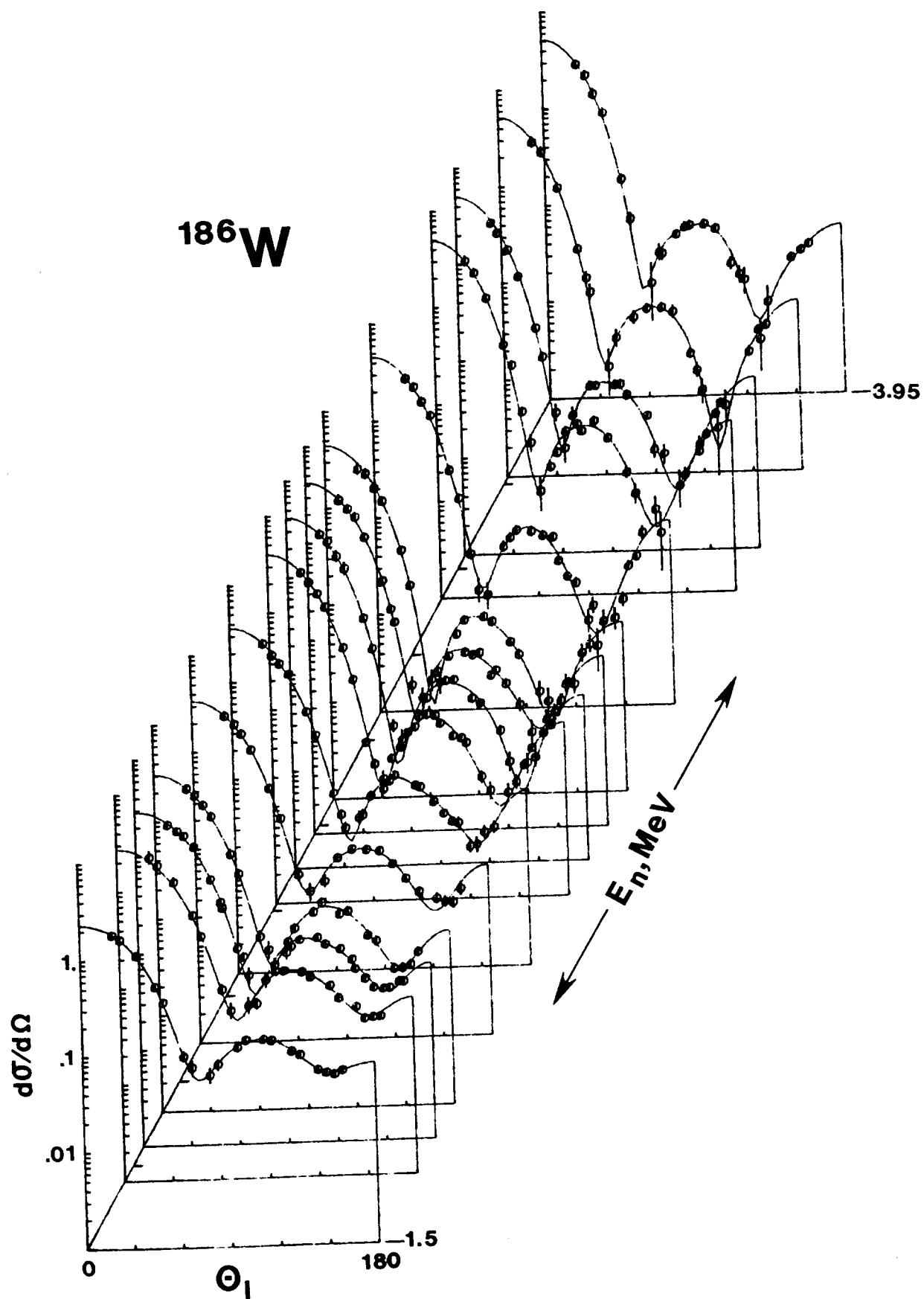


Fig. III-5C.

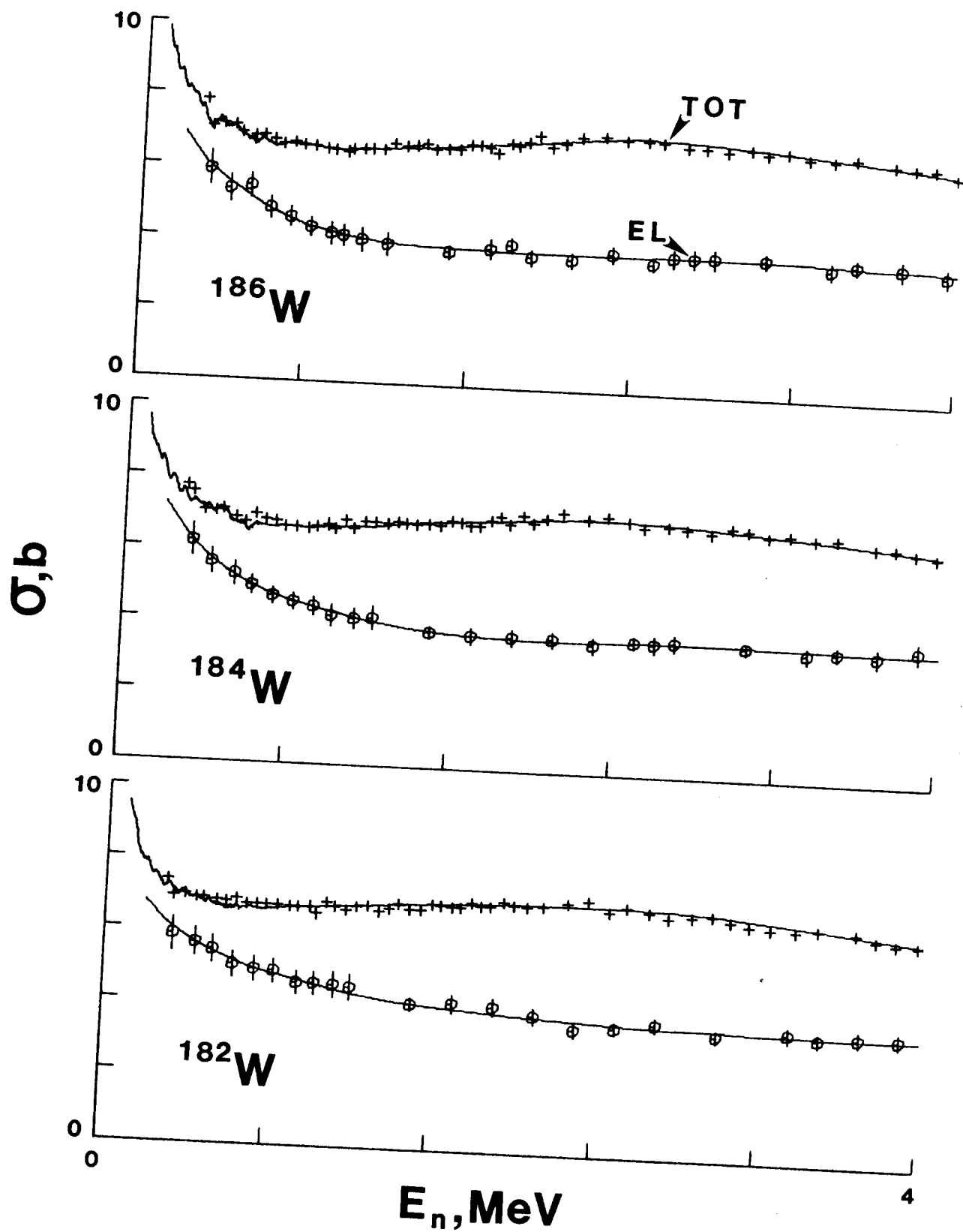


Fig. III-6.

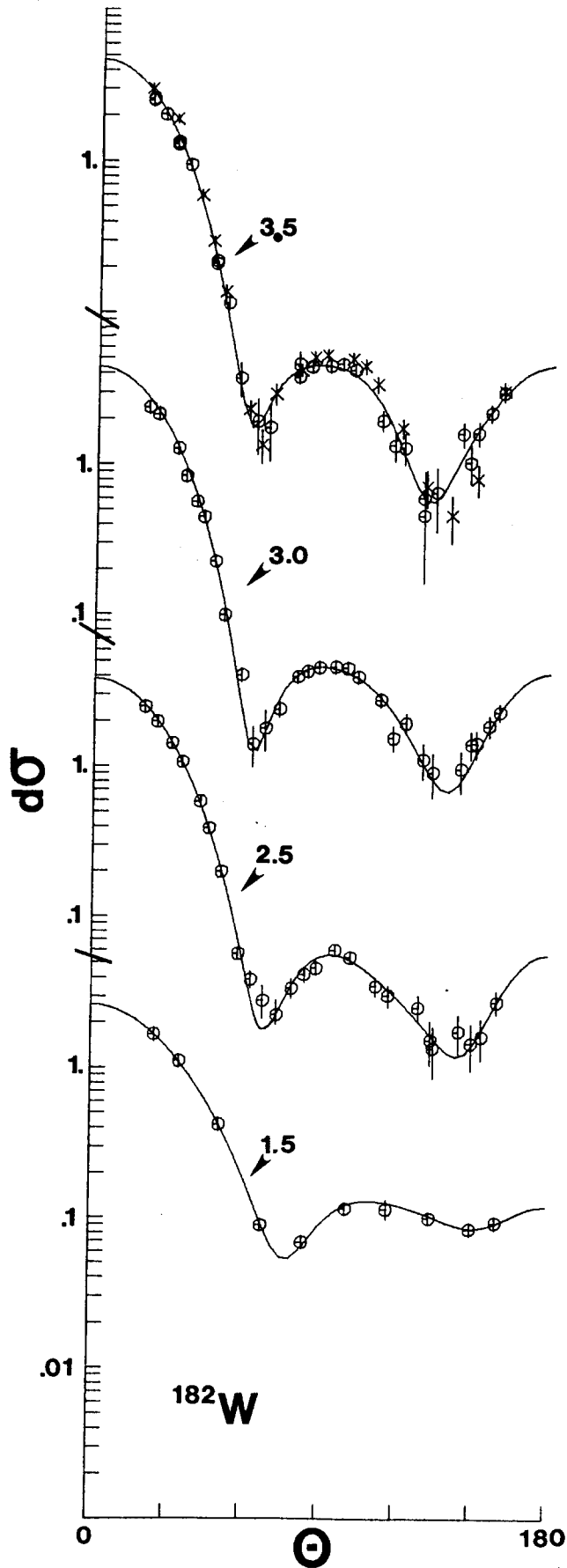


Fig. III-7A.

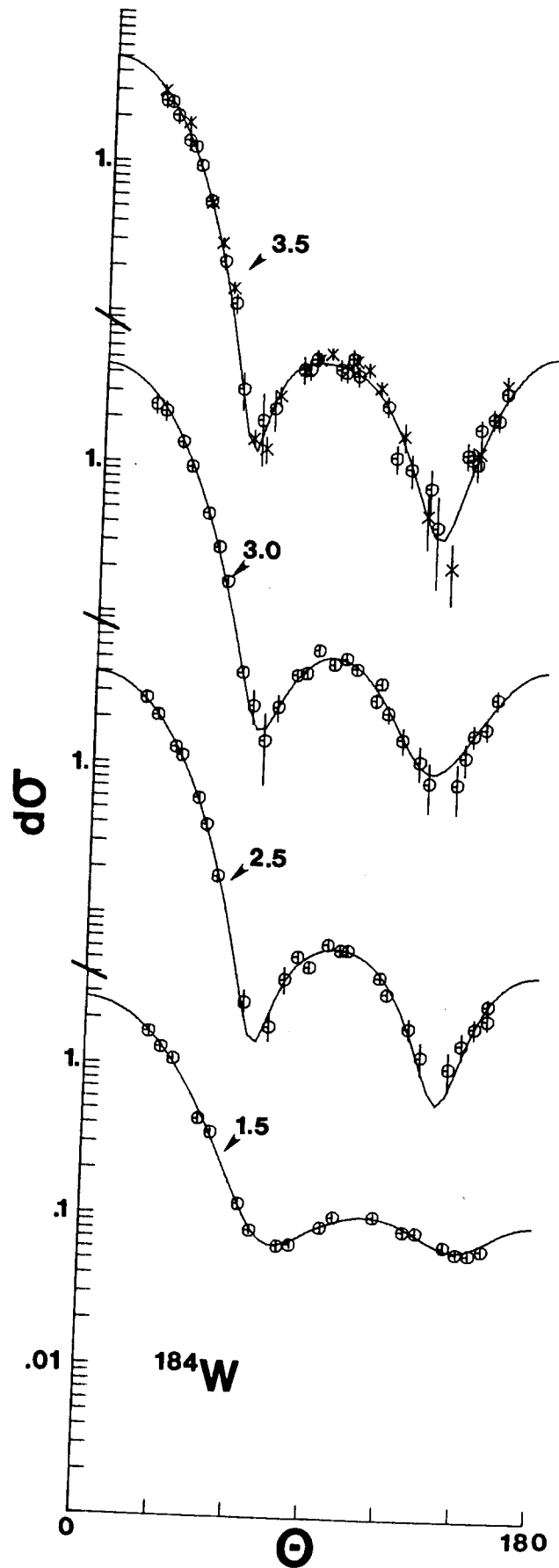


Fig. III-7B.

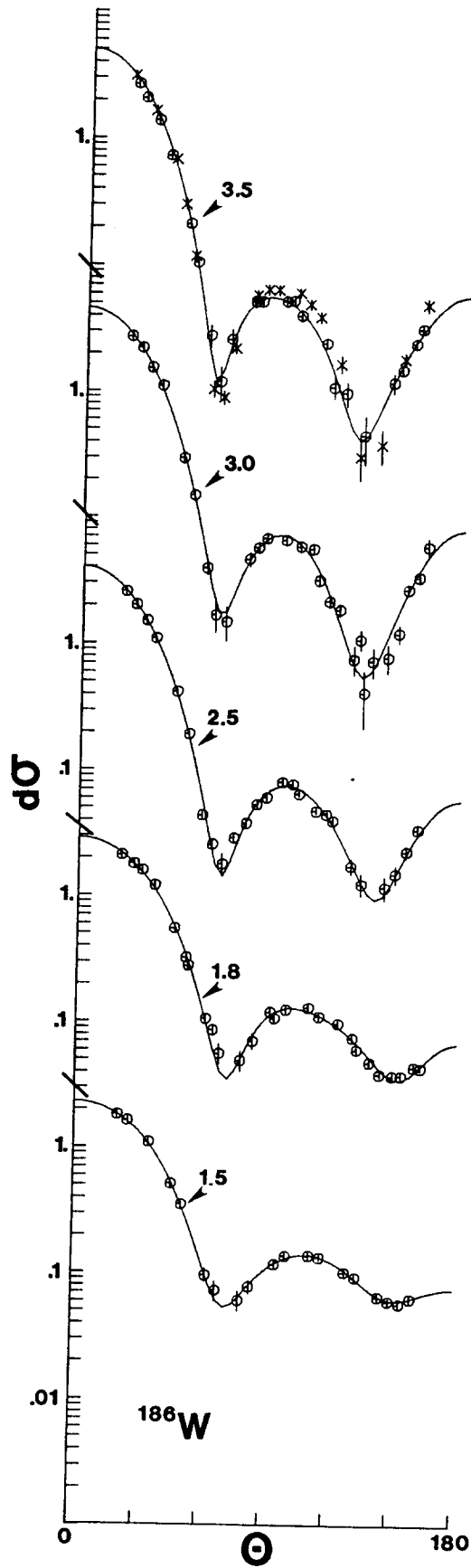


Fig. III-7C.

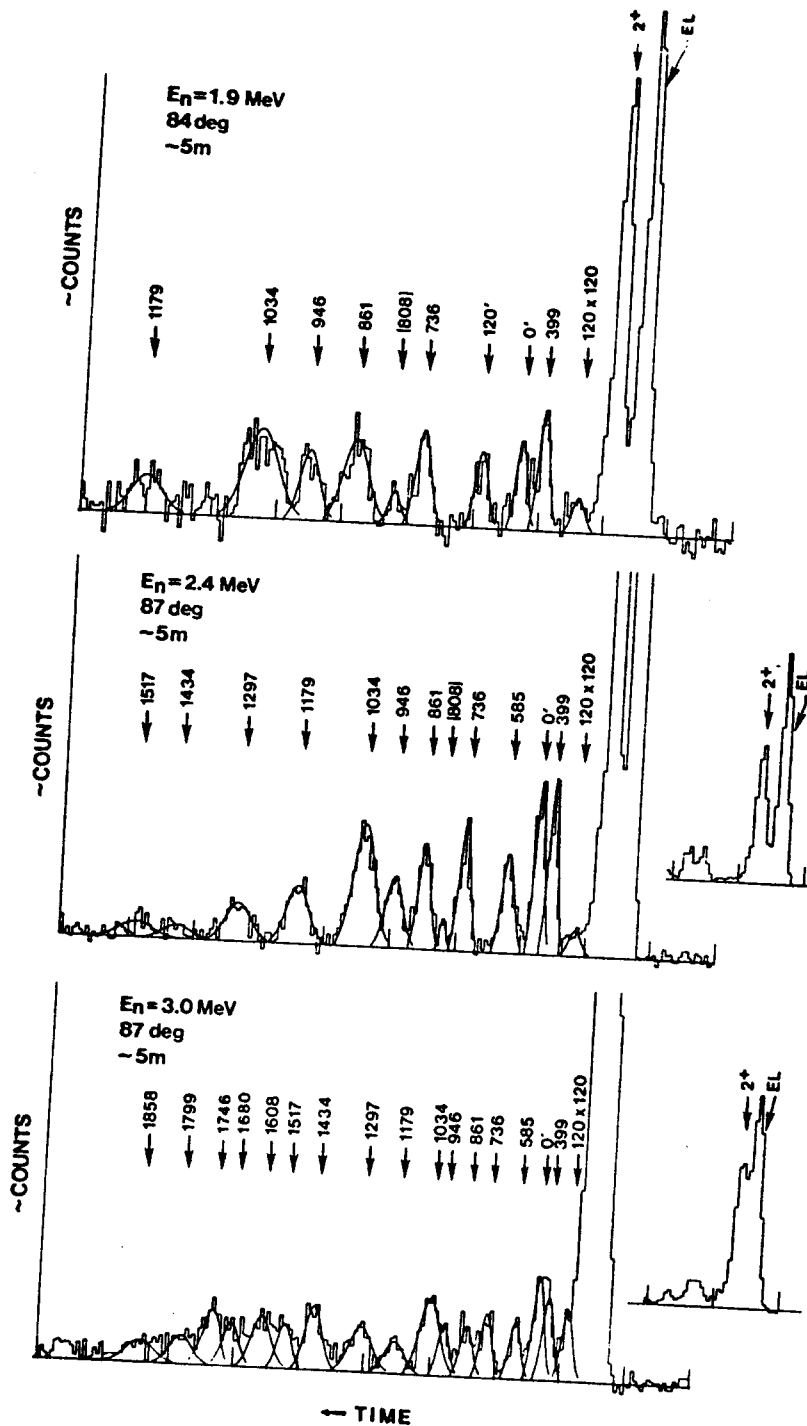


Fig. III-8.

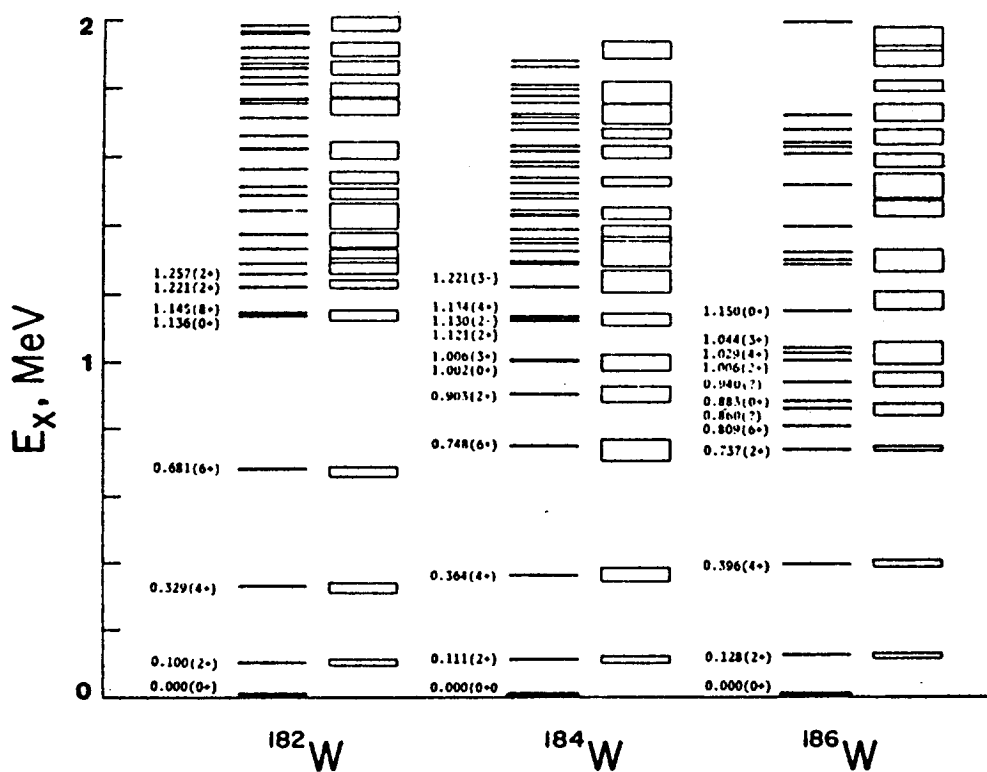


Fig. III-9.

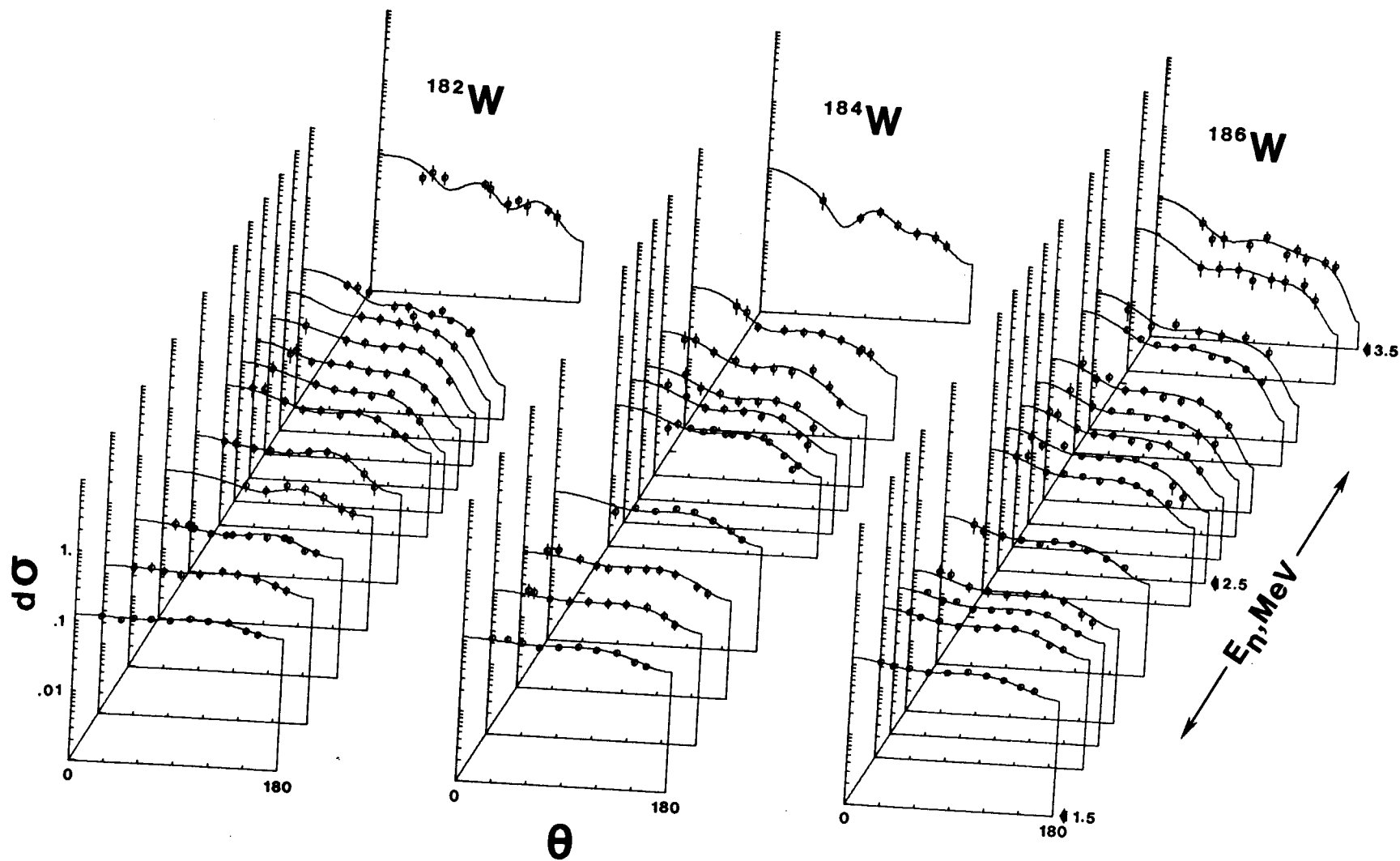


Fig. III-10.